Journal of Medicinal Chemistry

Article

pubs.acs.org/jmc

Design and Synthesis of Conformationally Constrained Inhibitors of Non-Nucleoside Reverse Transcriptase

Robert Gomez,*,† Samson J. Jolly,† Theresa Williams,† Joseph P. Vacca,† Maricel Torrent,‡ Georgia McGaughey,‡ Ming-Tain Lai,§ Peter Felock,§ Vandna Munshi,§ Daniel DiStefano,∥ Jessica Flynn,∥ Mike Miller,⊥ Youwei Yan,# John Reid,# Rosa Sanchez,∞ Yuexia Liang,∞ Brenda Paton,∞ Bang-Lin Wan,∞ and Neville Anthony†,●

Departments of †West Point Discovery Chemistry, ‡Chemistry Modeling and Informatics, §In Vitro Pharmacology, ∥Vaccine Research, ⊥ID Antiviral HIV Discovery, #Structural Chemistry, and ∞DMPK Preclinical WP, Merck Research Labs., 770 Sumneytown Pike, P.O. Box 4, West Point, Pennsylvania 19486-0004, United States

ABSTRACT: Highly active antiretroviral therapy (HAART) significantly reduces human immunodeficiency virus (HIV) viral load and has led to a dramatic decrease in acquired immunodeficiency syndrome (AIDS) related mortality. Despite this success, there remains a critical need for new HIV therapies to address the emergence of drug resistant viral strains. Next generation NNRTIs are sought that are effective against these mutant forms of the HIV virus. The bound conformations of our lead inhibitors, MK-1107 (**1**) and MK-4965 (**2**), were divergent about the oxymethylene linker, and each of these conformations was rigidified using two isomeric cyclic constraints. The constraint derived from the bioactive conformation of **2** provided novel, highly potent NNRTIs that possess broad spectrum antiviral activity and good pharmacokinetic profiles. Systematic SAR led to the identification of indazole as the optimal conformational constraint to provide MK-6186 (**3**) and MK-7445 (**6**). Despite their reduced flexibility, these compounds had potency comparable to that of the corresponding acyclic ethers in both recombinant enzyme and cell based assays against both the wild-type and the clinically relevant mutant strains.

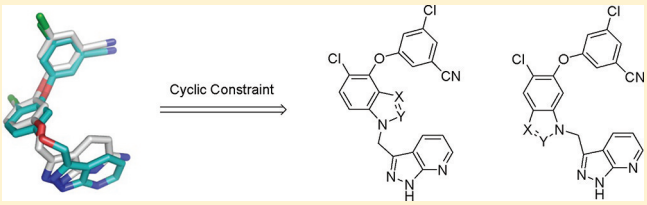

INTRODUCTION

HIV has a high rate of mutation due to its infidelity during replication. As a result, single drug therapy is not found to be durable because of the rapid selection of resistant mutant strains.[1−3] HAART significantly reduces HIV viral load and has led to a dramatic decrease in AIDS related mortality and a better quality of life for patients.[4] HAART typically combines at least two anti-HIV drugs simultaneously, as this greatly reduces the probability of the virus developing drug resistance.[5] The emergence of HIV-1 strains resistant to at least one antiretroviral drug highlights the need for further development of antiviral agents with improved efficacy against the mutant strains that are observed clinically.[6,7]

Reverse transcriptase (RT) inhibitors block the conversion of single stranded viral RNA to double stranded proviral DNA, a prerequisite to integration into host DNA.[8] NNRTIs interact with the RT enzyme at an allosteric site and induce a change in the substrate binding site which interferes with its DNA polymerase activity.[9] This class of inhibitor has gained an increasingly important role in HAART therapy because of its high specificity and lack of mitochondrial toxicity which characterizes the nucleoside inhibitors (NRTI's).[10] However, because of their allosteric mechanism of action, a common consequence of NNRTI use is the emergence of drug resistant forms of HIV. The most predominant mutants selected by first generation NNRTI therapy are the K103N and the Y181C variants.[11,12] Next generation NNRTIs are sought that possess broad spectrum antiviral activity against key mutant strains (especially K103N and Y181C) and that also present a high genetic barrier to the selection of new drug resistant viral strains. Additionally, to facilitate patient compliance, a next generation NNRTI that is both efficacious with once daily dosing and amenable to fixed dose combination HAART regimens is highly desirable. The NNRTI TMC-125[13] has been approved by the FDA for twice daily oral dosing and has demonstrated activity toward a number of key clinical mutations. More recently, the more potent follow-up compound TMC-278[14] has been approved by the FDA to be administered orally once daily.

Tucker et al.[15] have previously reported a series of diaryl ethers that feature a pyrazolopyridine, as exemplified by MK-1107 (**1**) (Figure 1). This compound has excellent potency versus wild type (wt) and key mutant viruses. The X-ray crystal structure of **1** (magenta) bound to the K103N RT enzyme (PDB entry 3DRS) (Figure 2) shows that the terminal benzonitrile ring fills a large lipophilic pocket in the

Received: July 30, 2011
Published: October 10, 2011

 © 2011 American Chemical Society

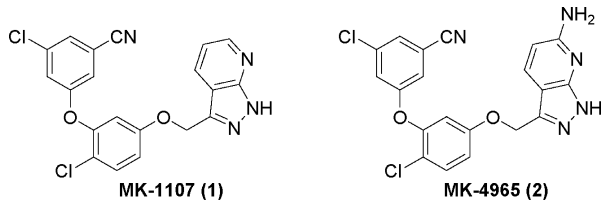

Figure 1. Lead structures.[15]

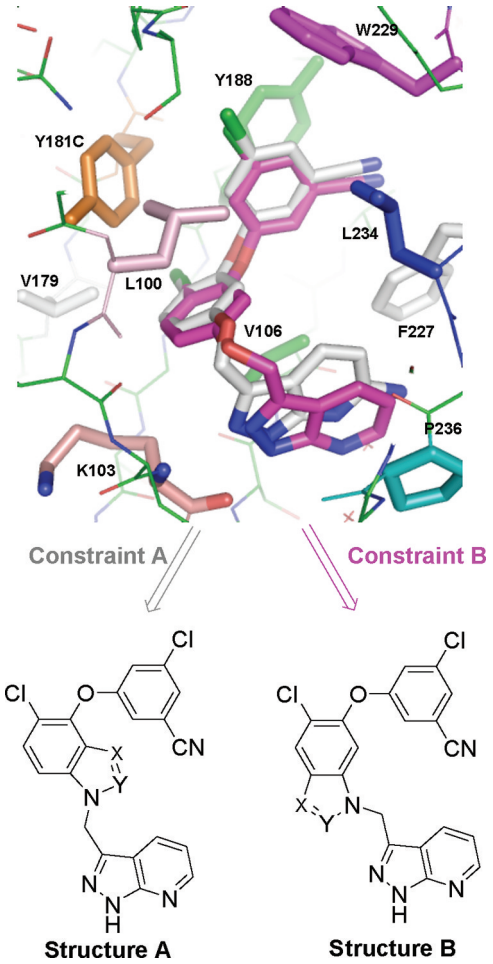

Figure 2. Bound conformation of **1** (magenta) superimposed with X-ray crystal structure of **2** (gray) in wt RT enzyme (PDB entry 3DRP).[15] This view shows select NNRTI binding site residues within 7 Å of ligand. Key active site residues are highlighted and labeled in black.

allosteric site formed by Y181−Y188−W229. Additionally, the central phenyl ring fits into a small lipophilic pocket formed by Y181−V179−V106. Importantly, key backbone hydrogen bond interactions between amino acid residue K103 and the pyrazole nitrogens are observed and may account for its persistent inhibition in the presence of the K103N mutant. A solvent exposed region can be accessed near this pyrazolopyridine ring, and water solubilizing groups have been added to the 6-position to affect the physical properties of compounds in this series which ultimately led to the 6-aminopyrazolopyridine, MK-4965 (**2**).

The crystal structure of the corresponding 6-amino analogue **2** bound to wt RT has also been determined (PDB entry 3DRP), and this molecule makes similar contacts with the enzyme. Interestingly, the cocrystal structures of **1** (magenta) and **2** (gray) present two distinct, divergent conformations about the oxymethylene linker (Figure 2). This prompted the speculation that each of these conformations might be reinforced by the introduction of appropriate cyclic constraints. Conformational rigidification is a commonly used strategy in drug design,[16,17] as it can lead to improved potency and selectivity while reducing the potential for drug metabolism. However, the consequence of rigidifying **1** and **2**, in terms of the effect on their antiviral profiles, was unclear, as it has been argued that conformational flexibility[13] is a necessary feature of broadly active NNRTIs.

After considering a variety of potential cyclic constraints of **1** and **2**, we envisioned that a fused five membered heteroaryl ring in which a nitrogen atom replaces the etheral oxygen atom would be a conservative way to evaluate this approach. The bound conformation of **2** can be rigidified with constraint A, while the bound conformation of **1** can be supported by constraint B (Figure 2). It was hypothesized that the increased steric hindrance and rigidity intrinsic to the ring constraints would reduce oxidative dealkylation of the pyrazolopyridine moiety which is a major metabolic clearance pathway for **1**.[15] Additionally, it was proposed that increasing the chemical diversity of these ring constraints by the incorporation of additional nitrogen atoms would lead to changes in physiochemical properties which would modulate both the potency and pharmacokinetic parameters of these molecules.

Triazoles **A** and **B** (X = N, Y = N, Figure 2), each derived from constraints A and B, respectively, were docked into the cognate site of RT (PDB entries 3DRP and 3DRS).[18] The resulting poses were compared with the bioactive conformations of **1** and **2** (Figures 3 and 4). The bioactive conformations

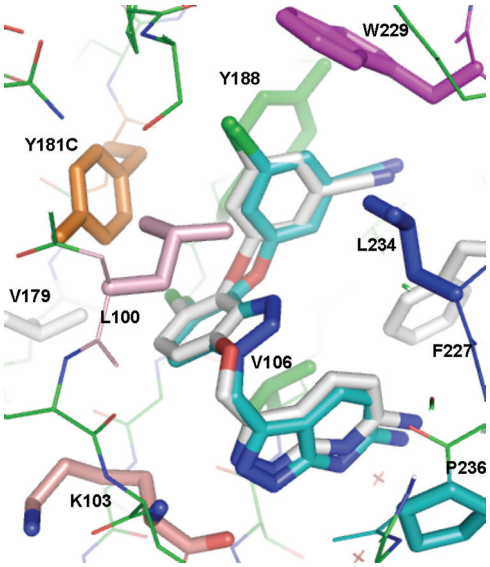

Figure 3. X-ray crystal structure of **2** (gray) bound to wt RT superimposed with the docked orientation of structure **A** (X, Y = N) (cyan). This view shows select NNRTI binding site residues within 7 Å of ligand. Key active site residues are highlighted and labeled in black.

of **1** and **2** showed that the oxygen of the oxymethylene linker is partially sp^3 hybridized and these linkers have measured dihedral angles of 40° and 32°, respectively, relative to the central phenyl ring. The nitrogen atoms of the modeled triazoles **A**

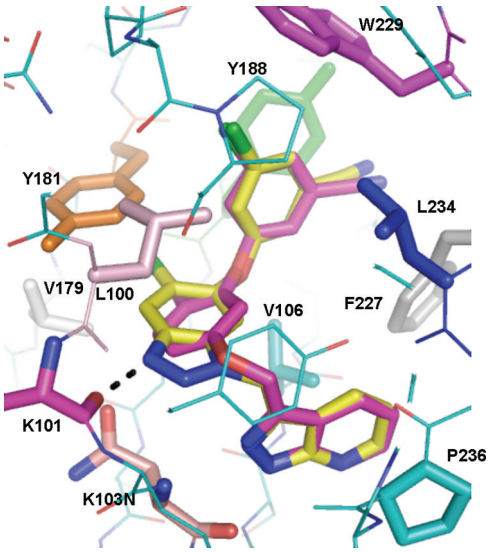

Figure 4. X-ray crystal structure of **1** (magenta) bound to K103N RT (PDB code 3DRS) superimposed with the docked orientation of structure **B** (X, Y = N) (yellow). This view shows select NNRTI binding site residues within 7 Å of ligand. Key active site residues are highlighted and labeled in black.

and **B**, however, are sp^2 hybridized resulting in linkages that are coplanar with the central phenyl ring. Despite these differences, the modeled triazole constraints A and B orient the terminal pyrazolopyridine and benzonitrile rings so that they maintain the key interactions with the enzyme.

The increased steric environment brought about by the ring constraint A appears to be accommodated in the cognate site of RT as shown by the docked model of triazole **A** (X = N, Y = N) in wt RT (Figure 3). The proximal residues of RT include L100 and Y318. L100 is 3.8 Å from the constraint, while the hydroxyl of Tyr318 is 3.5 Å distal and has the potential to form hydrogen bonds with heteroatoms at the 2-position of the constraint. Visual inspection of the docked conformation of structure **A** as a benzimidazole (X = N, Y = CH) reveals a potential non-bonding interaction between the 2-position of the benzimidazole and the 4-position of the pyrazolopyridine (Figure 5). This interaction was anticipated

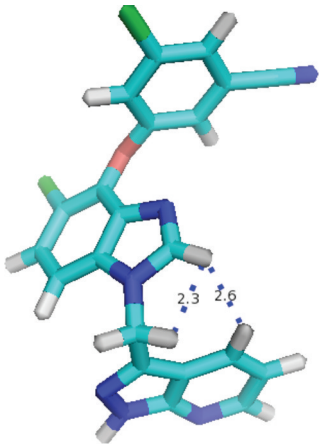

Figure 5. Structure **A** modeled in bioactive conformation of **2** showing the potential steric interactions with the 2-hydrogen.

to limit additional substitution at this position. Thus, computational studies were carried out to quantitate the effects of increased steric bulk at this position. Structure **A** compounds where the 2-position (Y) comprised N, C−H, and C−Me were each docked in the cognate site of RT. The ligand energy of each of these bioactive conformations was compared to the energy of the lowest energy conformer for each compound in vacuum, and these values are summarized in Table 1. The

Table 1. Ligand Energies Illustrating Effect of 2-Substitution of Ring Constraint

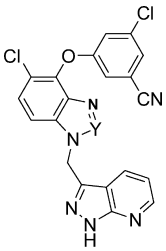

Structure **A**

Y	ligand energy, bound to wt RT (kcal/mol)	low energy conformer, vacuum (kcal/mol)	Δenergy (kcal/mol)
N	78.06	69.47	8.59
C−H	80.83	69.91	10.92
C−Me	85.63	71.71	13.92

change in energy (ΔE) between the bioactive conformation and the low energy conformation in vacuum provides an estimate of the amount of energy needed to attain the bioactive conformation. The ΔE for the methylbenzimidazole (Y = C−Me, 13.9 kcal/mol) is 5.3 kcal/mol higher than the ΔE for the 2-aza compound (Y = N, 8.6 kcal/mol). In addition, the ΔE of the benzimidazole (Y = C−H, 10.9 kcal/mol) was 2.3 kcal/mol higher than the 2-aza compound (Y = N, 8.6 kcal/mol), suggesting that even a hydrogen at this position would significantly impact the ability of these compounds to access the bioactive conformation and was predicted to lead to less potent inhibition of RT.

The increased steric environment brought about by ring constraint B, on the other hand, appears to be less well accommodated in the cognate site of RT as shown by the docked model of triazole **B** (X = N,Y = N) in wt RT (Figure 4). The proximal residues of RT to this constraint include K101 and K102. The carbonyl oxygen of K101 is only 2.4 Å from the constraint, while the α-carbon of K102 is 2.8 Å from the constraint. These potential nonbonded interactions with the constraint suggest that success with constraint B is dependent on the inherent flexibility of the enzyme[13] to accommodate this additional steric requirement. In addition, the docked model of triazole **B** shows a 20° tipping of the core ring, resulting in a 1.6 Å displacement of the chloro group relative to the corresponding group in the crystal structure of **1**. This tipping was required in order to maintain the important interactions of the protein with the terminal rings but is expected to be detrimental to binding. For these reasons, constraint A was considered more viable and was evaluated in more detail.

■ RESULTS AND DISCUSSION

Data for the compounds from the cyclic constraint A series is summarized in Table 2. Compounds were evaluated for

Table 2. Enzyme Inhibition and Antiviral Activity of 1 and 2 and Constraint Analogues 3−11

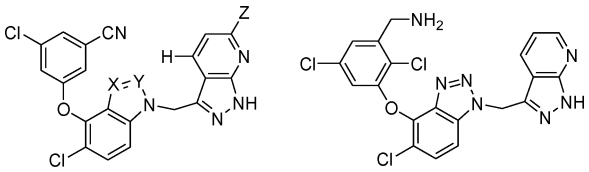

General structure 5

compd	X	Y	Z	inhibition of RT, K_i (nM)[a] wt	K103N	Y181C	antiviral activity in cell culture, CIC_{95} (nM)[b] wt	K103N	Y181C	wt 50% NHS
1[c]			H	0.12 ± 0.03	0.22 ± 0.04	0.23 ± 0.02	10 ± 0.6	15 ± 1.3	22 ± 2.1	52 ± 4.2
2[c]			NH_2	0.20 ± 0.01	0.39 ± 0.01	0.39 ± 0.02	4.9 ± 0.3	12 ± 1.0	27 ± 1.6	26 ± 1.5
3	CH	N	H	0.34 ± 0.05	0.58 ± 0.04	0.60 ± 0.04	11 ± 1.1	15 ± 1.6	58 ± 7	64 ± 6.1
4	N	N	H	0.24 ± 0.02	0.43 ± 0.04	0.44 ± 0.02	4.3 ± 0.6	3.8 ± 0.8	18 ± 6	23 ± 2.0
5	N	N	H	2.2	4.3	4.2	57	232 ± 23	418 ± 104	281 ± 59
6	CH	N	NH_2	0.61 ± 0.06	1.7 ± 0.2	1.9 ± 0.2	4.1 ± 0.3	9.7 ± 1.6	68	43 ± 5
7	N	N	NH_2	1.1 ± 0.6	0.94	1.2	3	5.8	37 ± 2	36 ± 2
8	N	CH	H	2.0 ± 0.8	5.3	3.3	23	66 ± 17	320 ± 57	390 ± 225
9	NH	C═O	H	>300	>600	>300	>833	>833	ND	>833
10	N	CMe	H	>300	>600	>300	>833	>833	ND	>833
11	CCl	N	H	46	28	42	>500	>2000	>2000	>5000

[a]Compounds were evaluated in a standard SPA assay. Values are the geometric mean of at least two determinations. All individual values are within 2-fold of the mean. The standard error of the mean is included for compounds with ≥3 determinations. ND = not determined. Assay protocols are detailed in ref 19. [b]CIC_{95} (cell culture inhibitory concentration) is defined as the concentration at which the replication of virus is inhibited by >95% in MT-4 human T-lymphoid cells maintained in RPMI 1640 medium containing either 10% FBS or 50% NHS. Values are the geometric mean of at least two determinations. All individual values are within 2-fold of the mean. The standard error of the mean is included for compounds with ≥3 determinations. Details of the assay protocol are provided in ref 20. ND = not determined. No cytotoxicity was observed for any of the compounds up to the upper limit of the assay (8.3 μM). [c]Oxyether linker. See Figure 1 for structures.

intrinsic enzyme inhibitory potency[19] versus wt RT as well as the K103N and Y181C mutant variants. Inhibitors were also evaluated for antiviral potency[20] and measured as the cell inhibitory concentration that blocks 95% of cell replication (CIC_{95}) against wt and the key mutant viruses in the presence of 10% fetal bovine serum (FBS) and with 50% normal human serum (NHS) to evaluate the effects of protein binding.

Incorporation of a nitrogen atom at the 2-position of the constraint to minimize the potential steric repulsion with the C−H bond at the 4-position of pyrazolopyridine led to the indazole **3**. This ring constraint resulted in a 2- to 3-fold reduction in intrinsic enzyme inhibition of both wt and the K103N and Y181C mutants relative to the lead oxyether **1**. Indazole **3** was, however, equipotent to **1** in cell culture against both wt and K103N mutant viruses but was 3-fold less active against the Y181C mutant. Incorporation of an additional nitrogen atom at the 3-position of the ring constraint provided the benzotriazole **4**. This compound was slightly more potent than the indazole **3** in the enzyme assays and was significantly (3- to 4-fold) more potent in the cell based assays.

Unfortunately, attempts to obtain X-ray structural information of either indazole **3** or benzotriazole **4** bound to wt RT were not successful, presumably because of their limited aqueous solubility. The crystal structure of **2** bound to RT (PDB entry 3DRP) reveals that the nitrile group occupies a solvent exposed region of the enzyme. Reduction of this nitrile group on a chloro analogue of **4** provided the aminomethyl derivative **5**. The improved physical properties of **5** facilitated ligand exchange and provided an X-ray crystal structure of **5** complexed with wt RT at a resolution of 2.6 Å (PDB entry 3T19).[21] Comparison of the bound conformation of **5** from this X-ray crystal structure with the crystal structure of **2** in wt RT (PDB entry 3DRP) shows high similarity between the structures (Figure 6) and is consistent with the previously

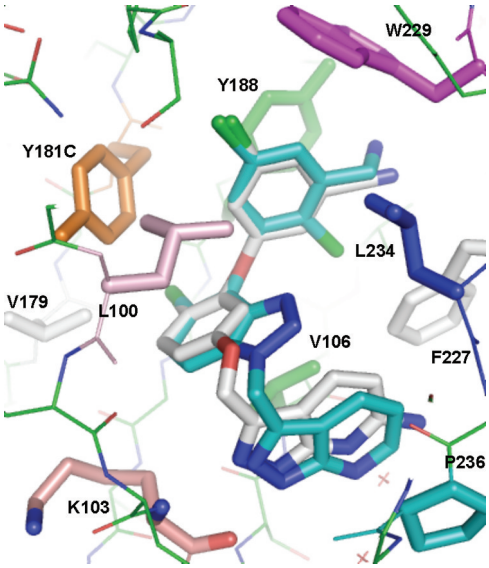

Figure 6. Bound conformation of **5**[21] (aqua) overlaid with crystal structure of **2** (gray) in wt RT.[15] This view shows select NNRTI binding site residues within 7 Å of ligand. Key active site residues are highlighted and labeled in black.

described docking studies (Figure 3).[18] The Y181 side chain orientation in this structure is analogous to the orientation of

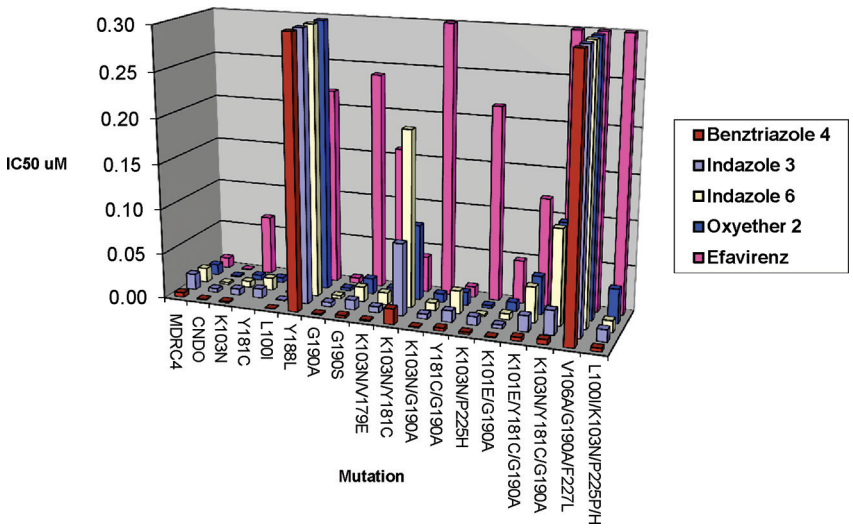

Figure 7. Antiviral potency of key compounds versus panel of isolated clinical viruses. Compounds were analyzed in a Monogram Bioscience Phenoscreen assay in the presence of FBS. The IC_{50} is defined as the concentration of compound in cell culture required to block 50% of viral replication. Values are derived from the average of two determinations, and all individual values are within 30% of the mean. Details are provided in ref 24. MDRC4 refers to a multidrug resistant virus. CNDO refers to a wild type virus.

this side chain observed for the ethers **1** and **2** (Figure 2). This conformation of Y181 has been observed previously[15,22] and provides an explanation for the maintainance of good potency in the presence of the Y181C mutation. Despite requisite realignment in the core ring, the key interactions with the protein residues that comprise the NNRTI binding site are preserved including the backbone hydrogen bond interactions between K103 and the pyrazole nitrogen atoms of the pyrazolopyridine group. Interestingly, NNRTIs containing an indazole central ring that is unsubstituted on the N1 nitrogen[23] are observed to bind in the opposite orientation compared to the compounds described here. Hydrogen bonding of the N1 hydrogen atom to the K101 backbone carbonyl is responsible for this alternative binding mode.

The pyrazolopyridine of **5** occupies the solvent exposed region outlined by P236 and suggests that the corresponding 6-amino group would be tolerated in accord with the findings with oxyether **2**. The 6-amino group was incorporated onto indazole and benzotriazole scaffolds to yield the more water-soluble derivatives **6** and **7**. As anticipated, **6** and **7** had potent antiviral activity in cell culture similar to **3** and **4** against both wt and the K103N and Y181C mutants.

Incorporation of a basic heterocycle into the cyclic constraint was evaluated in the context of the more basic and polar benzimidazole **8**. Consistent with the computational studies, introduction of even a hydrogen atom at the 2 position of the constraining scaffold leads to diminished potency in both enzyme inhibition (3- to 10-fold) and antiviral activity in cell culture (2- to 4-fold) relative to the indazole **3**. Importantly, the increased polarity of benzimidazole **8** leads to an increase in protein binding, as indicated by a larger shift in antiviral activity in the presence of NHS. As anticipated by our computational studies, substitution at the 2 position of the benzimidazole **8** to give the benzimidazol-2-one **9** and the 2-methylbenzimidazole **10** results in a complete loss of enzyme inhibition and antiviral activity. This demonstrates that the higher energetic cost associated with each ligand's ability to access the bioactive conformation correlates with the observed loss of inhibitory potency.

The impact of introducing a substituent at the 3 position of the cyclic constraint was also evaluated. Examination of the docked analogues of structure **A** in wt RT (Figure 3) suggested that there is ample room in the binding site to accommodate substitution at this position. Surprisingly, the 3-chloro substituted indazole **11** is 10-fold less active than the parent indazole **3**, perhaps because of a sterically induced reorientation of the benzonitrile ring.

The conformationally constrained inhibitors **3**, **4**, and **6** were evaluated for their antiviral potency against a more extensive panel of viruses from clinical isolates.[24] The activity profiles of these constrained inhibitors compared to the more flexible oxymethylene **2** and the preferred first generation NNRTI inhibitor efavirenz (EFV) are shown in Figure 7. Inhibitors **2**, **3**, **4**, and **6** had markedly improved profiles relative to efavirenz (magenta). All four inhibitors possess broad spectrum activities against the mutant viruses tested. The notable exceptions to this activity include the rare single mutation Y188L (occurs in 0.6% of clinical isolates).[25] This is presumably due to disruption of the π stacking interactions between the benzonitrile ring, which is common to each of these compounds, and the aryl ring of the Y188 residue. Each of these compounds was also ineffective against the triple mutation, V106A/G190A/F227L, presumably in part because of the loss of the hydrophobic interaction between the V106 side chain and the central phenyl ring of the ligands. The indazole **6** (yellow) showed an overall activity profile comparable to that of **2** (blue) but was 2-fold less potent against the virus containing the K103N/Y181C double mutant. Indazole **3** (purple) showed a profile comparable to that of **2** (blue) against the viruses that contained single and double mutations and improved activities against the viruses that contained the triple mutations. The benzotriazole **4** (brown) had the best profile and showed marked improvement in potency against many of the viruses with double and triple mutations. These results demonstrate that despite their more rigid nature, these conformationally constrained inhibitors retain activity against a broad panel of mutant viruses and that the observed activity profiles are comparable to those of their more flexible oxyether counterparts.

Our attention then turned to evaluation of the alternative constraint B. Within this context, the constraint B analogues benzotriazole **12** and the benzimidazole **13** were prepared, and the enzyme inhibitory and the antiviral activity potencies are shown in Table 3. Both **12** and **13** were significantly less active (50- to >1000-fold) than the corresponding alternatively constrained analogues **4** and **8**. Clearly the enzyme lacks the flexibility required to accommodate these heterocycles. Interestingly and in support of this interpretation, the ring opened intermediate **14**, while lacking the cyclic constraint, is considerably more potent. This improved activity may result from a realignment of the core benzene ring to produce a new hydrogen bonding interaction between the 4-amino group and the backbone carbonyl of the K101 residue.

Table 3. Enzyme Inhibition and Antiviral Activity of Constraint B Analogues 12−14

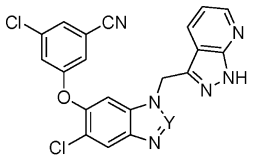

General Structure

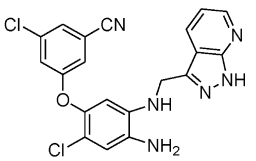

14

compd	Y	inhibition of RT, K_i (nM)[a]			antiviral CIC_{95} (nM)[b]	
		wt	K103N	Y181C	wt	K103N
12	N	>300	>300	>900	>833	>833
13	CH	114	>100	>100	693	732
14[c]		2.3	3.8	3.3	24	40

[a]Compounds were evaluated in a standard SPA assay. All values for **12** and **13** are from at least two determinations. The nonqualified value for **13** is the geometric mean of two determinations. Assay protocols are detailed in ref 19. [b]CIC_{95} (cell culture inhibitory concentration) is defined as the concentration at which the spread of virus is inhibited by >95% in MT-4 human T-lymphoid cells maintained in RPMI 1640 medium containing either 10% FBS or 50% NHS. All values for **12** and **13** are from at least two determinations. The nonqualified values for **13** are the geometric mean of two determinations. Details of the assay protocol are provided in ref 20. No cytotoxicity was observed for any of the compounds up to the upper limit of the assay (8.3 μM). [c]The values for **14** are from single determinations.

The pharmacokinetic parameters of key compounds were determined in rats and dogs and are tabulated in Table 3. Sprague−Dawley rats received an intravenous (iv) dose as a solution in DMSO via an in-dwelling canula implanted in the jugular vein or an oral dose as a suspension in aqueous methylcellulose. Similar procedures were used to evaluate pharmacokinetic parameters in dogs with the animals receiving iv and oral doses in a crossover fashion. Plasma concentrations of the indicated compounds were determined by liquid chromatography−mass spectrometry analysis, and the absolute oral bioavailability was determined by comparing the oral dose normalized area under the plasma concentration vs time curve (nAUC) with the iv nAUC.

The pharmacokinetics of the indazole **3** are characterized by a large volume of distribution (V_d of 10.5 and 6.0 L/kg), a moderate plasma clearance (Cl_p of 18 and 6.1 mL min^{-1} kg^{-1}), and long half-lives ($t_{1/2}$ of 7.6 and 12.8 h) in rats and dogs compared to the unconstrained oxymethylene ether **1** (Table 4). Despite its limited water solubility (<0.1 μg/mL at pH 2), **3** had good bioavailability (F of 76% and 48%) following oral dosing in rat and dog. The corresponding oxymethylene ether **1** had similarly limited water solubility (<0.1 μg/mL at pH 2) but poor oral bioavailability. Incorporation of the solubilizing 6-amino group onto the pyrazolopyridine moiety in **1** to give **2** was shown[15] to improved water solubility (10 μg/mL at pH 2) and increase bioavailability following oral dosing. The 6-amino analogue **6** was likewise more water-soluble (40 μg/mL) than **3** (<0.1 μg/mL) at pH 2 but was similarly poorly soluble (<0.1 μg/mL) at pH 7. Despite being more soluble at acidic pH, **6** had similar bioavailability and exposure with respect to **3** in both rat and dog. This suggests that low solubility does not significantly limit the absorption of indazole **3** and is consistent with absorption of both compounds occurring in the intestinal tract at sites of higher pH. It is interesting to note that the effect of constraining the oxymethylene ether **1** to the indazole **3** leads to a >10-fold increase in exposure whereas this increased exposure was not realized in the context of the corresponding the 6-amino derivatives **2** and **6**.

Table 4. Pharmacokinetics of the Oxymethylene Leads 1 and 2 and Key Cyclically Constrained Leads 3, 4, 6, 7, and 8[a]

	V_d, L/kg		Cl_p, mL min^{-1} kg^{-1}		$t_{1/2}$, h		F, %		nAUC (po) μM·h	
compd	rat	dog	rat	dog	rat	dog	rat	dog	rat	dog
1[b]	5.3	2.6	28	8.9	4.1	11.8	7.5	3	0.1	0.14
2[c,d]	2.0	1.7	9	5.8	3.5	3.9	52	47	2.3	3.1
3	10.5	6.0	18	6.1	7.6	12.8	76	48	1.6	2.3
4	5.5	1.3	14	1.6	4.8	11.3	7.3	9.5	0.18	0.45
6[e]	2.5	2.0	4.7	7.6	6.3	2.8	39	32	3.64	1.33
7[f]	4.4	0.65	11.9	2.2	4.7	12.8	<1	nd	0.02	nd
8	3.3	0.37	25.6	2.2	2.4	12.8	36	nd	0.56	nd

[a]Average of at least two Sprague−Dawley rats dosed at 10 mpk po (Methocel suspension) and 2 mpk iv (DMSO) unless otherwise noted. All values are within 25% of the mean. Average of at least two beagle dogs dosed at 2 mpk po (Methocel suspension) and 1mpk iv (DMSO) unless otherwise noted. nd = not determined. [b]Average of two beagle dogs dosed at 1 mpk po (Methocel suspension) and 0.25 mpk iv (DMSO). [c]Average of four Spraque−Dawley rats dosed at 10 mpk po (Methocel suspension) and 3 mpk iv (DMSO). [d]Average of three beagle dogs dosed at 10 mpk po (Methocel suspension) and 2 mpk iv (DMSO). [e]Average of two beagle dogs dosed at 2 mpk po (Methocel suspension) and 0.5 mpk iv (DMSO). [f]Average of three beagle dosed dosed at 0.125 mpk iv (DMSO) as part of a cassette dosing protocol.

The benzotriazole **4** has both lower volumes of distribution and lower clearances relative to indazole **3**, which results in comparable half-lives. However, despite the presence of an additional heteroatom, benzotriazole **4** retains poor water solubility (<0.1 μg/mL at pH 2). Contrary to indazole **3**, the permeability of benzotriazole **4** was presumably insufficient to overcome its poor aqueous solubility and resulted in low exposures. The 6-aminobenzotriazole **7** had an iv pharmacokinetic profile very similar to that of the parent **4** and, despite the solubilizing amino group, had negligible bioavailability.

The effect of introducing a more basic heterocycle into the constraining scaffold was examined for its effects on solubility and pharmacokinetic behavior. The more basic benzimidazole **8** (pK_a = 3.7 [26]) is likely to be protonated in the stomach, which results in increased water solubility (10 μg/mL at pH 2). However, this compound had a smaller volume of distribution and a higher plasma clearance in rat than the corresponding

Scheme 1[a]

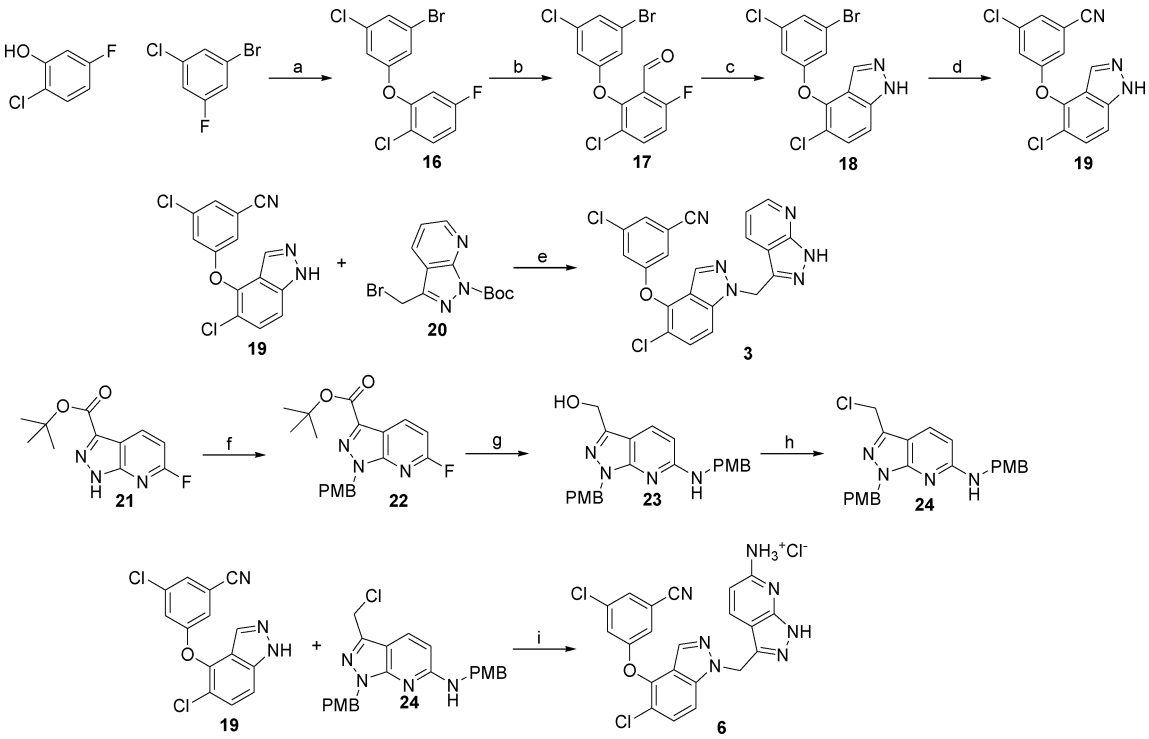

[a]Reagents and conditions: (a) K_2CO_3, NMP, 140 °C, 18 h, 65%; (b) LDA, THF, −78 °C, then DMF, 72%; (c) hydrazine hydrate, EtOH, 95°C, 4 days, 64%; (d) $Zn(CN)_2$, $Pd(PPh_3)_4$, DMF, 90 °C, 1 h, 89%; (e) Cs_2CO_3, DMF, then TFA, 36% (+20% 2-isomer); (f) KO^{t}Bu, PMB-Br, DMF, 68% (+22% isomer); (g) (i) PMB-NH_2, NMP, 80 °C, 3 h; (ii) LAH, THF, 0 °C to room temp, 84% (two steps); (h) thionyl chloride, CHCl3, 94%; (i) (i) LiO^{t}Bu, DMF, 0 °C to room temp; (ii) TFA reflux; (iii) HCl, $CHCl_3$/MeOH, 50% (+40% 2-isomer).

indazole **3**, which resulted in lower exposure following oral administration.

The two constrained analogues that had the best overall combination of activity and pharmacokinetic profiles were the indazoles **3** and **6**. Both of these inhibitors have pharmacokinetics in rat and dog that suggests a potential for once daily dosing in humans.

■ CHEMISTRY

The synthesis of the indazole **3** was carried out as shown in Scheme 1. S_NAr reaction of 1-bromo-3-chloro-5-fluorobenzene with 2-chloro-5-fluorophenol at 140 °C in NMP gave the requisite biaryl ether **16**. The key step in this synthesis was a fluoride directed deprotonation of **16** with LDA which, followed by quenching with DMF, gave the aldehyde **17** regioselectively. This aldehyde was reacted with excess hydrazine to afford the core indazole **18**. Palladium catalyzed cyanation afforded the key indazole **19**. This intermediate was alkylated with the bromide **20** in DMF using Cs_2CO_3 as base to provide a mixture of 1- and 2-substituted indazoles. However, this reaction was complicated by a transfer of the Boc protecting group from **20** to provide Boc protected **19** along with bis and tris alkylated byproducts. Fortunately, this mixture of products could be deprotected with TFA and purified by chromatography to give a 36% yield of the desired N1 derivative **3** along with 20% of the undesired N2 isomer. Compound **6** was similarly prepared by alkylation of the lithium anion of indazole **19** with the bis PMB protected chloride **24**. This mixture was purified by chromatography and deprotected in refluxing TFA to give **6**.

Synthesis of compounds **4** and **7**−**10** are outlined in Scheme 2. The key transformation of this sequence was a vicarious amination[27] of the nitrobenzene **25** to give a 1:1 mixture of regioisomeric aniline products that were readily purified to give a 36% yield of **26** and 37% yield of **27**. The nitroaniline **27** was reduced to the diaminobenzene **28** with tin(II) chloride in refluxing ethanol. Cyanide displacement of this bromide was unsuccessful under a variety of conditions, so it became necessary to form the heterocycles first and cyanate subsequently. All four heterocycles were prepared from this versatile diamine intermediate. Treatment of an acetic acid solution of the bisaniline **28** with sodium nitrite gave the benzotriazole **29**. The benzimidazole **30** was formed by heating **28** to 100 °C in formic acid. Treatment of **28** with triphosgene with pyridine as base provided the benzimidazole-2-one **31**. The 2-methylbenzimidazole **32** was synthesized by treating diamine **28** with acetic acid at 100 °C. Heteroaryls **29**−**32** were each cyanated using zinc cyanide in the presence of catalytic palladium tetrakistriphenylphosphine to give **33**−**36**. Heterocycles **33**−**36** were then each alkylated with bromide **20** using Cs_2CO_3 in DMF to form a regioisomeric mixture of products which were deprotected with TFA and purified to form the benzotriazole **4**, the benzimidazole **8**, the benzimidazole-2-one **9**, and the 2-methylbenzimidazole **10**. Additionally, the lithium salt of benzotriazole **33** was alkylated with the bis PMB protected chloride **24**. The resulting regioisomeric mixture was purified by chromatography, and the resulting bis PMB intermediate was deprotected in refluxing TFA to give triazole analogue **7**.

The syntheses of constraint B compounds **12** and **13** are outlined in Scheme 3. The synthesis takes advantage of the

Scheme 2[a]

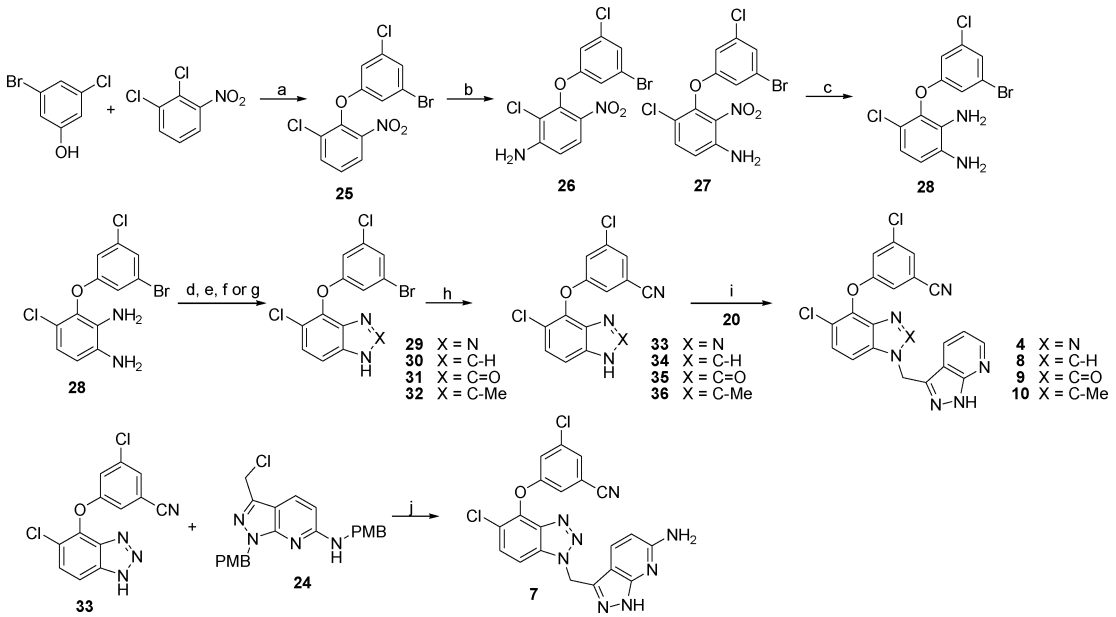

[a]Reagents and conditions: (a) K_2CO_3, NMP, 120 °C, 2 h, 85.4%; (b) KO^{t}Bu, $NH_2NMe_3^+I^-$, cat. CuI, DMF, 0−20 °C, 37% (+36% isomer); (c) $SnCl_2$, EtOH, 75 °C, 95%; (d) $NaNO_2$, AcOH, 95%; (e) HCO_2H, 100 °C, 1 h, 100%; (f) triphosgene, pyridine, DCM, 0 °C, 20 min, 67%; (g) AcOH, 100 °C, 6 h, 99%; (h) $Zn(CN)_2$, $Pd(PPh_3)_4$, DMF, 90 °C, 69−80%; (i) Cs_2CO_3, DMF, then TFA, 7−43%; (g) (i) LiO^{t}Bu, DMF, 0 °C to room temp; (ii) TFA reflux, 35%.

Scheme 3[a]

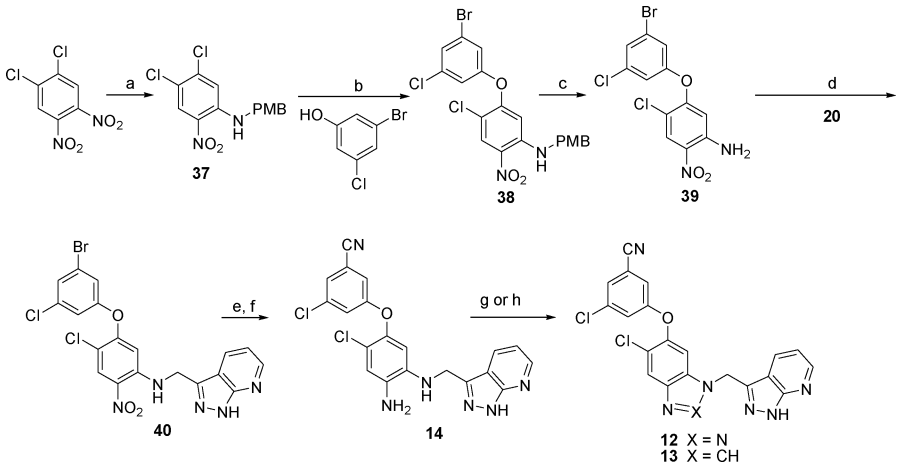

[a]Reagents and conditions: (a) PMB-NH_2, toluene, reflux, 99%; (b) K_2CO_3, NMP, 80 °C, 1 h, 74%; (c) TFA, 75 °C,100%; (d) Cs_2CO_3, DMF, then TFA, 32%; (e) $Zn(CN)_2$, $Pd(PPh_3)_4$, DMF, 95 °C, 2 h, 80%; (f) $SnCl_2$ H_2O, EtOH, reflux; (g) $NaNO_2$, HOAc; (h) HCO_2H, 50 °C, 2 h.

chemoselective displacement of an activated nitro group over a similarly activated chloro group. Specifically, reaction of the symmetrical 1,2-dinitro-4,5-dichlorobenzene with PMB amine gave only the nitro displaced adduct **37** in 99% yield. S_NAr displacement of the activated para chloride atom with 3-bromo-5-chlorophenol gave **38** in 74% yield. This PMB protected amine was treated with TFA to afford the nitroaniline **39**. This compound was alkylated with **20** to give a mixture of starting aniline **39**, desired alkylation product **40**, and some of the corresponding bis alkylation product. This mixture was purified by chromatography to give a 32% yield of **40**. The nitro group was reduced with tin(II) chloride in refluxing ethanol to give the differentially alkylated diamine **14**. This common intermediate was treated with sodium nitrite to form the benzotriazole **12** and with formic acid at 50 °C to form the benzimidazole **13**.

■ DISCUSSION AND CONCLUSIONS

The bound conformations of the acyclic oxyether NNRTIs **1** and **2** in RT were reinforced by two types of cyclic conformational constraints. Constraint B, which constrains the molecule to a conformation seen in oxymethylene ether **1** bound to the K103N mutant form of RT, gave only modest inhibition of reverse transcriptase presumably because of steric interactions with the residues surrounding the NNRTI binding pocket of the enzyme. In contrast, constraint A, which was

designed to preorganize the molecule in a manner that mimics the bound conformation of oxymethylene ether **2**, provided potent inhibitors with activity profiles that are similar to their more flexible acyclic counterparts. The indazole **3** and the benzotriazole **4** derived cores demonstrated the most potent enzyme inhibition and broadest spectrum of antiviral activity. The more water-soluble 6-aminopyrazolopyridine analogues, **6** and **7**, were prepared in analogy to the oxymethylene series and were found to be equipotent to **3** and **4**. The indazoles **3** and **6** had good pharmacokinetic profiles in rats and dogs and offer potential for once daily dosing in humans. These compounds provide a combination of excellent pharmacokinetic profiles, potent enzyme inhibition, and broad spectrum antiviral activities. As such, **3** and **6** were selected as preclinical development candidates and designated MK-6186 and MK-7445, respectively. Further details of the clinical development of these compounds including formulation, pharmacokinetic characterization, and process chemistry optimization will be presented in subsequent publications from our laboratories.

■ EXPERIMENTAL SECTION

Silica gel flash chromatography was performed on an ISCO Combiflash Companion unit using prepacked ISCO RediSep silica gel cartridges. Reverse phase chromatographic separations were performed on a Gilson automated HPLC system using Luna C18, 10 μm, 100 Å columns. ^{1}H NMR spectra were routinely obtained on a 400 MHz Varian FT NMR spectrometer and are referenced versus TMS. NMR solvents used were $CDCl_3$, CD_3OD, or DMSO-d_6 as indicated. Chemical shifts are reported in δ units relative to the internal standard TMS. LC−MS was performed using a Waters Alliance 2695/Micromass ZQ LC/MS system with a YMC Pro C18 5 μm/120 Å, 3 mm × 50 mm cartridge and a 95:5 A/B gradient (A = 92% water/8% ACN/0.05% TFA; B = 100% ACN/0.0425% TFA) over 4 min at a flow rate of 2 mL/min, with UV (215 or 254 nm) and mass detection. Retention times and purity assessments for all final compounds are reported from a second HPLC method using a Thermo Separations system with a YMS Pro C18 S-5 120 Å, 4.6 mm × 33 mm cartridge and a 95:5 gradient (A = water/0.1% TFA, B = ACN/0.085% TFA) over 5 min at a flow rate of 1 mL/min with UV (215 and 254 nm) detection. All compounds were assessed at >95% purity by both analytical methods. Electrospray (ES) and atmospheric pressure chemical ionization (APSI) accurate mass spectral data were acquired by use of a Bruker Daltonics 7 T Fourier transform ion cyclotron resonance (FTICR) spectrometer. External calibration was accomplished with oligomers of polypropylene glycol. Aldrich Sure-Seal solvents were used when anhydrous solvents were necessary. All reactions were carried out under inert atmosphere (argon or nitrogen).

3-Bromo-5-chlorophenyl 2-chloro-5-fluorophenyl ether (16). To a solution of 2-chloro-5-fluorophenol (82.3 g, 562 mmol) and 1-bromo-3-chloro-5-fluorobenzene (124 g, 590 mmol) in NMP (200 mL) was added K_2CO_3 (155 g, 1.123 mol). The resulting mixture was then heated to 140 °C for 30 h, after which the mixture was poured into water (1500 mL) and the aqueous layer extracted with EtOAc (2500 + 1500 mL). The combined extracts were washed with water and brine. The solvent was removed in vacuo and the resulting residue was distilled under high vacuum at 135−190 °C to give **16** (121.24 g, 64.3%) as a clear, colorless liquid. ^{1}H NMR ($CDCl_3$): δ 7.45 (dd, 1H, J = 9.0 and 4.5 Hz), 7.28 (t, J = 1.7 Hz, 1H), 7.26 (s, 1H), 7.00 (t, 1 h, J = 1.95 Hz), 6.92 (ddd, J = 10.5, 7.6, and 2.7 Hz, 1H), 6.89 (t, J = 1.95 Hz, 1H) ppm.

2-(3-Bromo-5-chlorophenoxy)-3-chloro-6-fluorobenzaldehyde (17). To a solution of **16** (100 g, 298 mmol) in THF (300 mL) cooled to −78 °C over a dry ice/acetone bath was added 1.8 M lithium diisopropylamide in hexanes/THF/ethylbenzene (174 mL, 313 mmol) over 10 min. The resulting mixture was stirred for 20 min and then treated with DMF (46.1 mL, 595 mmol). This mixture was then removed from the cooling bath and allowed to warm to room temperature and kept at room temperature for 1 h. The reaction was then quenched with water (1000 mL), and the aqueous layer was extracted with EtOAc (3 × 500 mL). The combined extracts were washed with water (500 mL), dried over $MgSO_4$ and the solvent removed in vacuo. This residue was purified on a silica gel column (0−40% CH_2Cl_2/hexanes) to give **17** (77.51 g, 71.5%) as a clear liquid. ^{1}H NMR ($CDCl_3$): δ 10.22 (s, 1H), 7.72 (dd, J = 5.6 and 9.0 Hz, 1H), 7.24 (m, 1H), 7.15 (dd, J = 9 Hz, 1H), 6.88 (t, J = 1.7 Hz, 1H), and 6.77 (t, J = 1.7 Hz, 1H) ppm. LRMS (M − 18 + 1) = 346.7

4-(3-Bromo-5-chlorophenoxy)-5-chloro-1*H*-indazole (18). To a suspension of **17** (77.5 g, 213 mmol) in EtOH (120 mL) was added hydrazine hydrate (31 mL, 639 mmol). The resulting mixture was then heated at reflux for 4 days, after which time the mixture was cooled to room temperature, diluted with water (100 mL) and the resulting solid was filtered. The solid was preabsorbed onto silica gel (300 g) and purified on a silica gel (1500 g) column (0−40% EtOAc/CH_2Cl_2) to give **18** (40.0 g, 52.3%) as a white solid. ^{1}H NMR ($CDCl_3$) δ 10.15 (br s, 1H), 7.80 (s, 1H), 7.48 (d, J = 8.8 Hz, 1H), 7.38 (d, J = 8.8 Hz, 1H), 7.24 (m, 1H), 6.98 (t, J = 1.7 Hz, 1H) and 6.86 (t, J = 1.7 Hz, 1H) ppm. LRMS (M + 1) = 358.8.

3-Chloro-5-[(5-chloro-1*H*-indazol-4-yl)oxy]benzonitrile (19). To a degassed suspension of **18** (40 g, 112 mmol) and $Zn(CN)_2$ (15.74 g, 134 mmol) in DMF (400 mL) was added palladium tetrakistriphenylphosphine (38.7 g, 33.5 mmol), and the mixture was heated to 90 °C for 1 h. After this time, the mixture was cooled to room temperature and partitioned between saturated aqueous NH_4Cl (500 mL), water (500 mL), and EtOAc (2 × 1000 mL). The combined extracts were dried over $MgSO_4$, absorbed onto silica gel (200 g), and the solvent was removed in vacuo. This solid was purified on a silica gel (1000 g) column (0−10% EtOAc/CH_2Cl_2) to give **19** (30.18 g, 89%) as a white solid. ^{1}H NMR ($CDCl_3$) δ 10.25 (br s, 1H), 7.82 (s, 1H), 7.49 (d, J = 8.8 Hz, 1H), 7.42 (d, J = 8.8 Hz, 1H), 7.36 (t, J = 1.5 Hz, 1H), 7.18 (t, J = 1.9 Hz, 1H), 7.02 (dd, J = 1.3 and 2.4 Hz, 1H) ppm. LRMS (M + 1) = 303.9.

3-Chloro-5-{[5-chloro-1-(1*H*-pyrazolo[3,4-*b*]pyridin-3-ylmethyl)-1*H*-indazol-4-yl]oxy}benzonitrile (3). To a suspension of **19** (24 g, 79 mmol) and *tert*-butyl 3-(bromomethyl)-1*H*-pyrazolo[3,4-*b*]pyridine-1-carboxylate (**20**) (24.63 g, 79 mmol) in DMF (150 mL) at 0 °C was added Cs_2CO_3 (51.4 g, 158 mmol). The resulting mixture was allowed to warm to room temperature and then stirred for 2 h. LC−MS shows 47% Boc protected **3**, 28.8% Boc protected 2-isomer. This mixture was partitioned between water (1000 mL) and EtOAc (1000 mL). The organic extract was washed with water (1000 mL) and then with brine (200 mL), dried over $MgSO_4$ and the solvent removed in vacuo. This residue was purified on a silica gel (500 g) column (0−10% ACN/CH_2Cl_2) to give Boc protected **3** and **3** (from deprotection on column). The Boc protected **3** was dissolved in TFA (50 mL) and allowed to stand at room temperature for 10 min, after which the solvent was removed in vacuo. The resulting solid and the previously isolated **3** were then preabsorbed onto silica gel (50 g) and purified on a silica gel (330 g) column (10−30% ACN/CH_2Cl_2) to give **3** (12.2 g, 35.6%) as a white solid. ^{1}H NMR (DMSO-d_6): δ 13.65 (s, 1H), 8.49 (d, J = 4.6 Hz, 1H), 7.91 (d, J = 8.3 Hz, 1H), 7.89 (s, 1H), 7.82 (d, J = 8.8 Hz, 1H), 7.62 (d, J = 8.6 Hz, 1H), 7.47 (m, 1H), 7.39 (m, 1H), 7.13 (dd, J = 7.7 and 4.6 Hz, 1H), and 6.05 (s, 2H) ppm. HRMS: measured m/z, $[M + H]^+$ = 435.0514 (theoretical, 435.0522). LC purity 99.99%; t_R = 3.754 min.

2-(3-Bromo-5-chlorophenoxy)-1-chloro-3-nitrobenzene (25). 2,3-Dichloronitrobenzene (34.2 g, 178 mmol), 3-bromo-5-chlorophenol (46.2 g, 223 mmol), and K_2CO_3 (61.6 g, 445 mmol) were suspended in NMP (200 mL) and placed in an oil bath at 120 °C for 2 h. The mixture was allowed to cool to room temperature. Water (1000 mL) was added, and the aqueous layer was extracted with EtOAc (2 × 1000 mL). The combined organic extracts were washed with water (2 × 500 mL), dried over $MgSO_4$, filtered, and the solvent was evaporated in vacuo to a solid. This solid was recrystallized from EtOAc (200 mL) to give **25** (51.23 g, 63.2%) as a crystalline solid. The filtrate was further purified by chromatography on silica gel (330 g), eluting with 0−25% CH_2Cl_2/hexanes to yield additional **25** (18 g, 22.2%). ^{1}H NMR (CD_3CN) δ 8.02 (dd, J = 1.5 and 8.3 Hz, 1H), 7.88

(dd, J = 1.6 and 8.2 Hz, 1H), 7.52 (dd, J = 8.2 and 8.3 Hz, 1H), 7.38 (m, 1H), 7.07 (m, 1H), and 6.97 (m, 1H) ppm.

3-(3-Bromo-5-chlorophenoxy)-4-chloro-2-nitroaniline (27). CuCl (5.45 mg, 0.055 mmol) and K_2CO_3 (247 mg, 2.204 mmol) were suspended in DMF (3 mL) at 0 °C and treated with 1,1,1-trimethylhydrazinium iodide (139 mg, 0.689 mmol). This mixture was allowed to stir over an ice bath for 5 min and then cooled to −40 °C. This mixture was treated dropwise with a solution of **25** (200 mg, 0.551 mmol) in DMF (3 mL). After 15 min, this mixture was quenched cold with aqueous saturated NH_4Cl (10 mL) and water (10 mL) and then allowed to warm to 25 °C. The aqueous layer was extracted with EtOAc (2 × 50 mL), and the combined extracts were washed with water (3 × 50 mL). The resulting organic layer was dried over $MgSO_4$, filtered and the solvent was removed in vacuo. This solid was adsorbed onto silica gel (500 mg) and purified by silica gel chromatography (0−25% EtOAc/CH_2Cl_2) to afford **26** (75.5 mg, 36%) and **27** (76.5 mg, 37%). **26**: ^{1}H NMR (CD_3CN) δ 7.98 (d, J = 8.5 Hz, 1H), 7.33 (dd, J = 2 Hz, 1H), 7.04 (dd, J = 2 Hz, 1H), 6.94 (dd, J = 2 Hz, 1H), 6.83 (d, J = 9.3 Hz, 1H), and 5.67 (br s, 2H) ppm. LRMS (M + 1) = 378.7. **27**: ^{1}H NMR (CD_3CN) δ 7.41 (d, J = 9.3 Hz, 1H), 7.35−7.32 (m, 1H), 7.07−7.05 (m, 1H), 6.98−6.95 (m, 1H), 6.90 (d, J = 9.3 Hz, 1H) and 5.87 (br s, 2H) ppm. LRMS (M + 1) = 378.7.

3-(3-Bromo-5-chlorophenoxy)-4-chlorobenzene-1, 2-diamine (28). Tin(II) chloride dihydrate (17.0 g, 75 mmol) and **27** (5.7 g, 15.1 mmol) were suspended in MeOH (100 mL) and heated to 75 °C. After 11 h, the mixture was allowed to cool to room temperature and the solvent was removed in vacuo. The resulting residue was diluted with EtOAc (150 mL), and 10% aqueous Na_2CO_3 (250 mL) was added with vigorous stirring until the pH was 10. The resulting white paste was filtered through diatomaceous earth and the pad rinsed with additional EtOAc (200 mL). The biphasic filtrate was separated and the aqueous layer extracted again with EtOAc (200 mL). The combined organic extracts were dried ($MgSO_4$), filtered and the solvent was removed in vacuo to yield **28** (4.97 g, 95%) as a solid. ^{1}H NMR (CD_3CN): δ 7.30−7.28 (m, 1H), 6.97−6.94 (m, 1H), 6.87−6.84 (m, 1H), 6.68 (d, J = 8.5 Hz, 1H), 6.59 (d, J = 8.5 Hz, 1H) ppm. LRMS (M + 1) = 348.8.

4-(3-Bromo-5-chlorophenoxy)-5-chloro-1*H*-benzotriazole (29). To a solution **28** (4.97 g, 14.28 mmol) in AcOH (25 mL) at 15 °C was added aqueous $NaNO_2$ (0.4M, 39.3 mL). The mixture was allowed to warm to room temperature. After 1.5 h, the mixture was diluted with EtOAc (300 mL), and the organic layer was separated and washed with water (3 × 100 mL). This extract was dried over $MgSO_4$, filtered and the solvent removed in vacuo to afford **29** (5.01 g, 98%) as a solid. ^{1}H NMR (DMSO-d_6) δ 8.14 −8. 00 (m, 1H), 7.86−7.54 (m, 2H), 7.50−7.46 (m, 1H), 7.20−7.14 (m, 1H), 7.12−7.04 (m, 1H) ppm.

3-Chloro-5-[(5-chloro-1*H*-1,2,3-benzotriazol-4-yl)oxy]-benzonitrile (33). A degassed suspension of **29** (5.00 g, 13.93 mmol), $Zn(CN)_2$ (1.96 g, 16.71 mmol), and palladium tetrakis-triphenylphosphine (4.83 g, 4.18 mmol) in dry DMF (50 mL) was heated to 90 °C for 2.5 h. After this time, the mixture was allowed to cool to room temperature, diluted with EtOAc (300 mL), washed with water (4 × 100 mL), dried over $MgSO_4$, and filtered. Silica gel (20 g) was added to the filtrate, and the solvent was removed in vacuo. This dry powder was purified using silica gel chromatography, eluting with 0−5% MeOH/CH_2Cl_2 to give **33** (3.83 g, 90%) as a solid. ^{1}H NMR (DMSO-d_6) δ 7.90−7.80 (m, 2H), 7.75−7.60 (m, 1H), 7.60−7.45 (m, 2H) ppm.

***tert*-Butyl 3-{[5-Chloro-4-(3-chloro-5-cyanophenoxy)-1*H*-1,2,3-benzotriazol-1-yl]methyl}-1*H*-pyrazolo[3,4-*b*]pyridine-1-carboxylate.** To a suspension of **33** (2.00 g, 6.55 mmol) and Cs_2CO_3 (2.14 g, 6.55 mmol) in DMF (15 mL) at room temperature was added **20** (1.84 g, 5.90 mmol) as a solution in DMF (5 mL). After the mixture was stirred for 1 h at room temperature, the reaction was quenched with aqueous NH_4Cl (20 mL). The mixture was diluted with water (10 mL), and the aqueous layer was extracted with EtOAc (3 × 75 mL). The combined organic extracts were washed with water (3 × 75 mL), dried over $MgSO_4$, filtered and the solvent removed in vacuo. The resulting residue was purified using silica gel chromatography, eluting with 25−50% EtOAc/hexanes to afford the title compound (1.10 g, 31%) as a white solid. ^{1}H NMR ($CDCl_3$): δ 8.72−8.70 (m, 1H), 8.15−8.12 (m, 1H), 7.96 (d, J = 9.0 Hz, 1H), 7.83 (d, J = 9.0 Hz, 1H), 7.82−7.80 (m, 1H), 7.58−7.54 (m, 2H), 7.45−7.41 (m, 1H), 6.47 (s, 2H), and 1.62 (s, 9H) ppm. LRMS (M + 1) = 435.7.

3-Chloro-5-{[5-chloro-1-(1*H*-pyrazolo[3,4-*b*]pyridin-3-ylmethyl)-1*H*-1,2,3-benzotriazol-4-yl]oxy}benzonitrile (4). *tert*-Butyl 3-{[5-chloro-4-(3-chloro-5-cyanophenoxy)-1*H*-1,2,3-benzotriazol-1-yl]methyl}-1*H*-pyrazolo[3,4-*b*]pyridine-1-carboxylate (1.10 g, 2.05 mmol) was dissolved in TFA (10 mL) at room temperature. After 5 min, the solvent was evaporated in vacuo to a solid. This was purified by silica gel chromatography, eluting with 0−5% MeOH/CH_2Cl_2 to afford **4** (752 mg, 84%) as a white solid. ^{1}H NMR ($CDCl_3$): δ 8.52−8.46 (m, 1H), 8.35 (d, J = 4.15 Hz, 1H), 7.59 (d, J = 8.79 Hz, 1H), 7.57 (d, J = 8.78 Hz, 1H), 7.36 (s, 1H), 7.33−7.27 (m, 1H), 6.98 (s, 1H), and 6.25 (s, 2H) ppm. HRMS: measured m/z, $[M + H]^+$ = 436.0467 (theoretical, 436.0475). LC purity 99.7%; t_R = 3.572 min.

1-{3-Chloro-5-[2-chloro-5-(1*H*-pyrazolo[3,4-*b*]pyridin-3-ylmethoxy)phenoxy]phenyl}methenamine (5). A solution of 2,5-dichloro-3-{[5-chlro-1-(1*H*-pyrozolo[3,4-*b*]pyridine-3-ylmethyl)-1*H*-1,2,3-benzotriazol-4-yl]oxy}benzonitrile (prepared as in **4**) (283 mg, 0.601 mmol) in THF (30 mL) was cooled to 0 °C over an ice bath, and to it was added 1 M LAH in THF (1.202 mL, 1.202 mmol). Then the mixture was removed from the cooling bath and stirred at room temperature for 1 h. After this time, the mixture was recooled over an ice bath and then quenched with EtOAc (50 mL) and allowed to warm to room temperature. This mixture was treated with saturated aqueous Na_2SO_4 and stirred for 10 min to give a white suspension. This suspension was treated with solid Na_2SO_4 until dry, and this suspension was filtered and the solvent removed in vacuo. This residue was purified by reverse phase preparative HPLC. The desired fractions were combined, and the solvent was removed in vacuo. This residue was partitioned between saturated aqueous Na_2CO_3 and CH_2Cl_2. The organic extract was dried over $MgSO_4$, filtered and the solvent removed in vacuo. This residue was redissolved in 4 M HCl in dioxane and the solvent was removed in vacuo to give **5** (82 mg, 27%) as a white solid. ^{1}H NMR ($CDCl_3$): δ 8.53 (d, J = 4.5 Hz, 1H), 8.12 (d, J = 8 Hz, 1H), 7.95 (br s, 3H), 7.89 (d, J = 9 Hz, 1H), 7.79 (d, J = 9 Hz, 1H), 7.48 (s, 1H), 7.21 (dd, 5 and 8 Hz, 1H), 6.92 (s, 1H), 6.39 (s, 2H), and 3.57 (s, 2H) ppm. HRMS: measured m/z $[M + H]^+$ = 474.0392 (theoretical, 474.0398). LC purity 97%; t_R = 2.372 min.

***tert*-Butyl 6-Fluoro-1-(4-methoxybenzyl)-1*H*-pyrazolo[3,4-*b*]pyridine-3-carboxylate (22) and *tert*-Butyl 6-Fluoro-2-(4-methoxybenzyl)-2*H*-pyrazolo[3,4-*b*]pyridine-3-carboxylate.** To a solution of **21** (29.55 g, 125 mmol) in THF (300 mL) cooled in an ice bath was added KO^{t}Bu (13.98 g, 125 mmol) at such a rate as to maintain the temperature between 5 and 10 °C. This mixture was treated with 4-methoxybenzyl bromide (18.2 mL, 125 mmol) and stirred over an ice bath for 1 h and then at 25 °C for 18 h. The resulting suspension was quenched with saturated aqueous NH_4Cl (200 mL) and then the aqueous layer extracted with EtOAc (2 × 300 mL). The combined organic extracts were washed with brine, dried over $MgSO_4$, and the solvent was removed in vacuo. The resulting residue was purified by chromatography using silica gel (1000 g), eluting with 0−30% EtOAc/hexanes to give *tert*-butyl 6-fluoro-2-(4-methoxybenzyl)-2*H*-pyrazolo[3,4-*b*]pyridine-3-carboxylate (9.75 g, 21.9%) and **22** (30.3 g, 68.2%) as white solids. **22**: ^{1}H NMR ($CDCl_3$): δ 8.44 (t, J = 8 Hz, 1H), 7.40 (d, J = 8.8 Hz, 2H), 6.90 (d, J = 8.8 Hz, 1H), 6.83 (d, J = 8.5 Hz, 2H), 5.61 (s, 2H), and 3.76 (s, 3H) ppm. LRMS (M + 1) = 380.1. *tert*-Butyl 6-fluoro-2-(4-methoxybenzyl)-2*H*-pyrazolo[3,4-*b*]pyridine-3-carboxylate: ^{1}H NMR ($CDCl_3$): δ 8.35 (t, J = 8.5 Hz, 1H), 7.43 (d, J = 8.5 Hz, 2H), 6.88 (d, J = 8.5 Hz, 1H), 6.82 (d, J = 8.5 Hz, 2H), 6.01 (s, 2H), and 3.76 (s, 3H) ppm. LRMS (M + 1) = 380.1.

{1-(4-Methoxybenzyl)-6-[(4-methoxbenzyl)amino]-1*H*-pyrazolo[3,4-*b*]pyridin-3-yl}methanol (23). To a solution of **22** (2.55 g, 7.14 mmol) in NMP (30 mL) was added 4-methoxbenzylamine (2.80 mL, 21.41 mmol), and the mixture was heated to 80 °C for 2 h. This mixture was allowed to cool to room temperature, diluted

with water (200 mL), and the aqueous layer was extracted with EtOAc (2 × 200 mL). The combined extracts were washed with water (100 mL), dried over $MgSO_4$, and filtered. Silica gel (17 g) was added, and the solvent was removed in vacuo. This solid was purified by chromatography using silica gel (80 g), eluting with 0−100% EtOAc/CH_2Cl_2 to give *tert*-butyl 1-(4-methoxybenzyl)-6-[(4-methoxybenzyl)amino]-1*H*-pyrazolo[3,4-*b*]pyridine-3-carboxylate. ^{1}H NMR ($CDCl_3$): δ 7.98 (d, J = 8.8 Hz, 1H), 7.33 (d, J = 8.8 Hz, 2H), 7.29 (d, J = 8.6 Hz, 2H), 6.86 (d, J = 8.6 Hz, 2H), 6.77 (d, J = 8.8 Hz, 2H), 6.36 (d, J = 8.8 Hz, 1H), 5.52 (s, 2H), 5.00 (t, J = 5.5 Hz, 1H), 4.61 (d, J = 5.5 Hz, 2H), 3.81 (s, 6H), and 1.54 (s, 9H) ppm. LRMS (M + 1) = 474.0.

To a solution of *tert*-butyl 1-(4-methoxybenzyl)-6-[(4-methoxybenzyl)amino]-1*H*-pyrazolo[3,4-*b*]pyridine-3-carboxylate (38.4 g, 81 mmol) in THF (300 mL) cooled over an ice bath was added 2 M LAH in THF (50 mL, 100 mmol) at such a rate to keep the temperature below 10 °C. The resulting mixture was stirred over an ice bath for 20 min and then allowed to warm to 25 °C for 4 h. This mixture was then recooled over an ice bath and treated sequentially with water (3.8 mL), 15% aqueous NaOH (3.8 mL), and water (11.4 mL) and then stirred for 30 min. The resulting suspension was filtered through diatomaceous earth, and the resulting cake was rinsed with more THF (300 mL). The combined filtrates were treated with silica gel (100 g), and the solvent was removed in vacuo. This preabsorbed solid was purified by chromatography using silica gel (500 g), eluting with 0−20% MeOH/CH_2Cl_2 to give **23** (23.6 g, 83% for two steps) as a white solid. ^{1}H NMR (DMSO-d_6): δ 7.73 (d, J = 9 Hz, 1H), 7.26 (d, J = 8 Hz, 2H), 7.21 (d, J = 8 Hz, 2H), 6.87 (d, J = 8 Hz, 4H), 6.41 (d, J = 9 Hz, 1H), 5.49 (t, 1H), 5.34 (s, 2H), 4.74 (d, J = 5.4 Hz, 2H), 4.45 (d, J = 5.4 Hz, 2H), and 3.72 (s, 6H) ppm. LRMS (M + 1) = 404.9.

3-(Chloromethyl)-*N*,1-bis(methoxybenzyl)-1*H*-pyrazolo[3,4-*b*]pyridin-6-amine (24). To a slurry of **23** (1.49 g, 3.68 mmol) in $CHCl_3$ (15 mL) cooled over an ice bath was added thionyl chloride (538 μL, 7.37 mmol). The resulting mixture was then allowed to warm to room temperature and left at room temperature for 30 min. The reaction was determined by LC/MS monitoring not to be complete, so the mixture was recooled over an ice bath and treated with additional thionyl chloride (100 μL) and then stirred at room temperature for 30 min. This mixture was poured into aqueous $NaHCO_3$ (50 mL), extraction was with $CHCl_3$ (100 mL), and the solvent was removed in vacuo. This residue was purified by chromatography using silica gel (120 g), eluting with 0−60% EtOAc/$CHCl_3$ to give **24** (1.46 g, 94%) as a white solid. ^{1}H NMR ($CDCl_3$): δ 7.76 (d, J = 8.8 Hz, 1H), 7.30 (d, J = 8.8 Hz, 2H), 7.26 (d, J = 8.8 Hz, 2H), 6.86 (d, J = 8.5 Hz, 2H), 6.79 (d, J = 8.8 Hz, 2H), 6.29 (d, J = 8.5 Hz, 1H), 5.41 (s, 2H), 5.00 (t, J = 5.8 Hz, 1H), 4.80 (s, 2H), 4.61 (d, J = 5.8 Hz, 2H), 3.80 (s, 3H), and 3.76 (s, 3H) ppm. LRMS (M + 1) = 422.9.

3-Chloro-5-{[5-chloro-1-({1-(4-methoxybenzyl)-6-[(4-methoxybenzyl)amino]-1*H*-pyrazolo[3,4-*b*]pyridin-3-yl}-methyl)-1*H*-indazol-4-yl]oxy}benzonitrile. A solution of **19** (9.0 g, 29.6 mmol) in DMF (75 mL) was treated with LiO^tBu (2.37 g, 29.6 mmol) and stirred for 5 min. This mixture was cooled over an ice bath and treated with a solution of **24** (12.77 g, 30.2 mmol) in DMF (75 mL). This mixture was stirred at 25 °C for 18 h. After this time, aqueous NH_4Cl (200 mL) was added and extracted with EtOAc (2 × 500 mL). The combined extracts were dried over $MgSO_4$, filtered, and the solvent was removed in vacuo. This residue was purified by chromatography using silica gel (330 g), eluting with 0−10% EtOAc/CH_2Cl_2 to give the title compound (11.49 g, 56.2%) and 3-chloro-5-{[5-chloro-2-({1-(4-methoxybenzyl)-6-[(4-methoxybenzyl)amino]-1*H*-pyrazolo[3,4-*b*]pyridin-3-yl}methyl)-2*H*-indazol-4-yl]oxy}-benzonitrile (8.23 g, 40.3%) as white solids. ^{1}H NMR ($CDCl_3$): δ 7.72 (s, 1H), 7.36−7.23 (m, 7H), 7.14 (m, 1H), 6.94 (m, 1H), 6.83 (d, J = 9.5 Hz, 2H), 6.81 (d, J = 8.8 Hz, 2H), 6.13 (d, J = 8.8 Hz, 1H), 5.78 (s, 2H), 5.44 (s, 2H), 4.94 (t, J = 5.6 Hz, 1H), 4.55 (d, J = 5.6 Hz, 2H), and 3.78 (s, 6H) ppm. LRMS (M + 1) = 691.8.

3-({1-[(6-Amino-1*H*-pyrazolo[3,4-*b*]pyridin-3-yl)methyl]-5-chloro-1*H*-indazol-4-yl}oxy)-5-chlorobenzonitrile (6). 3-Chloro-5-{[5-chloro-1-({1-(4-methoxybenzyl)-6-[(4-methoxybenzyl)amino]-1*H*-pyrazolo[3,4-*b*]pyridin-3-yl}methyl)-1*H*-indazol-4-yl]oxy}-benzonitrile (11.49 g, 16.64 mmol) was dissolved in TFA (100 mL) and placed in an oil bath at 75 °C for 2 h. This mixture was allowed to cool to room temperature, and the solvent was removed in vacuo. The resulting residue was suspended in $CHCl_3$/EtOAc (4:1, 1200 mL), and aqueous $NaHCO_3$ (500 mL) was added and vigorously stirred for 10 min. The layers were partitioned and the aqueous portion was back-extracted with $CHCl_3$/EtOAc (4:1, 1200 mL) and then EtOAc (2 × 1000 mL). The extracts were each washed with water (500 mL) and enough MeOH to keep them clarified. The combined extracts were dried over $MgSO_4$, filtered, and the solvent was removed in vacuo. The resulting residue was purified by chromatography using silica gel (330 g), eluting with 0−10% MeOH/$CHCl_3$ to give **6** (7.08 g, 95%) as a white solid. ^{1}H NMR (DMSO-d_6): δ 12.60 (s, 1H), 7.86 (s, 1H), 7.81−7.78 (m, 1H), 7.73 (d, J = 9.0 Hz, 1H), 7.58 (d, J = 9.0 Hz, 1H), 7.49−7.47 (m, 1H), 7.38−7.34 (m, 2H), 6.30 (s, 2H), 6.21 (d, J = 8.8 Hz, 1H), and 5.8882 (s, 2H) ppm. LRMS (M + 1) = 449.7.

3-{[5-Chloro-4-(3-chloro-5-cyanophenoxy)-1*H*-indazol-1-yl]-methyl}-1*H*-pyrazolo[3,4-*b*]pyridin-6-aminium chloride (6·HCl). To a warmed (40 °C) solution of **6** (7.08 g, 15.72 mmol) in 20% CH_3OH/$CHCl_3$ (1200 mL) was added 1 N HCl (15.72 mL, 15.72 mmol), and the resulting mixture was then concentrated in vacuo. This solid was azeotroped from ACN (3 × 200 mL) and dried under high vacuum overnight to give **6**·HCl (7.19 g, 94%) as a white solid. ^{1}H NMR (DMSO-d_6 with puff NH_3 vapor): δ 7.86 (s, 1H), 7.81 (t, J = 1.5 Hz, 1H), 7.73 (d, J = 9 Hz, 1H), 7.58 (d, J = 9 Hz, 1), 7.49 (dd, J = 1.5 Hz, 1H), 7.37 (d, J = 6 Hz, 1H), 7.36 (s, 1H), 6.30 (br s, 2H), 6.23 (d, J = 8.8 Hz, 1H), and 5.82 (s, 2H) ppm. HRMS: measured m/z, $[M + H]^+$ = 450.0623 (theoretical, 450.0631). LC purity 98.4%; t_R = 2.888 min.

3-Chloro-5-{[5-chloro-1-({2-(4-methoxybenzyl)-6-[(4-methoxybenzyl)amino]-2*H*-pyrazolo[3,4-*b*]pyridin-3-yl}-methyl)-1*H*-1,2,3-benzotriazol-4-yl]oxy}benzonitrile. The regioisomer of **24**, 3-(chloromethyl)-*N*,2-bis(4-methoxybenzyl)-2*H*-pyrzolo[3,4-*b*]pyridin-6-amine, was prepared analogously to **24** starting from *tert*-butyl 6-fluoro-2-(4-methoxybenzyl)-2*H*-pyrazolo-[3,4-*b*]pyridine-3 carboxylate. LiO^tBu (37 mg, 0.459 mmol) and **33** (140 mg, 0.459 mmol) were dissolved in DMF (1 mL), and the mixture was allowed to stir for 20 min. The mixture was then cooled over an ice bath, and a solution of 3-(chloromethyl)-*N*,2-bis(4-methoxybenzyl)-2*H*-pyrazolo[3,4-*b*]pyridine-6-amine (198 mg, 0.468 mmol) in DMF (1 mL) was added dropwise. After 1 h, the reaction was quenched with saturated aqueous NH_4Cl (3 mL). The mixture was diluted with water (3 mL), and the aqueous layer was extracted with EtOAc (2 × 25 mL). The combined organic extracts were washed with brine (4 × 10 mL), dried over $MgSO_4$, filtered, and the solvent was removed in vacuo. This residue was purified by chromatography using silica gel (12 g), eluting with 0−100% EtOAc/hexanes to give the title compound (135 mg, 42.5%) and the 2-isomer 3-chloro-5-{[5-chloro-2-({2-(4-methoxybenzyl)-6-[40methoxybenzyl)amino]-2*H*-pyrazolo[3,4-*b*]pyridine-3-yl}methyl)-2*H*-1,2,3-benzotriazol-4-yl]-oxy}benzonitrile. ^{1}H NMR (CD_3CN): δ 7.58 (d, J = 11 Hz, 1H), 7.53 (t, J = 1.5 Hz, 1H), 7.46 (d, J = 8.9 Hz, 1H), 7.32−7.25 (m, 4H), 7.17 (d, J = 8.9 Hz, 1H), 6.91−6.83 (m, 4H), 6.67 (d, J = 8.7 Hz, 2H), 6.45 (d, J = 9 Hz, 1H), 6.12 (s, 2H), 5.96 (br t, 1H), 5.44 (s, 2H), 4.53 (d, J = 6 Hz, 2H), 3.74 (s, 3H), and 3.70 (s, 3H) ppm. LRMS (M + 1) = 690.5.

3-({1-[(6-Amino-1*H*-pyrazolo[3,4-*b*]pyridin-3-yl)methyl]-5-chloro-1*H*-1,2,3-benzotriazol-4-yl}oxy)-5-chlorobenzonitrile (7). A solution of 3-chloro-5-{[5-chloro-1-({2-(4-methoxybenzyl)-6-[(4-methoxybenzyl)amino]-2*H*-pyrazolo[3,4-*b*]pyridin-3-yl}methyl)-1*H*-1,2,3-benzotriazol-4-yl]oxy}benzonitrile (135 mg, 0.195 mmol) in TFA (10 mL) was heated to 75 °C for 2 h. This mixture was allowed to cool to room temperature, and the solvent was removed in vacuo. The resulting residue was diluted with $CHCl_3$/EtOAc (4:1, 50 mL), and CH_3OH was added until a clear solution was achieved. This solution was washed with 50% aqueous Na_2CO_3 (10 mL), and the aqueous portion was back-extracted with $CHCl_3$ (25 mL). The combined extracts were dried ($MgSO_4$), filtered, and the solvent was removed in vacuo. This residue was preabsorbed onto silica gel (500 mg) and purified by chromatography using silica gel (12 g), eluting with 0−5% MeOH/CH_2Cl_2 to afford **7** (51 mg, 58%) as a white solid. ^{1}H NMR (DMSO-d_6) δ 7.82 (d, J = 9.0 Hz, 1H), 7.81 (m, 1H), 7.75

(d, J = 9.0 Hz, 1H), 7.58 (m, 1H), 7.55 (d, J = 8.8 Hz, 1H), 7.52 (m, 1H), 6.36 (br s, 2H), 6.30 (d, J = 8.8 Hz, 1H), and 6.16 (s, 2H) ppm. LRMS (M + 1) = 450.6.

3-{[5-Chloro-4-(3-chloro-5-cyanophenoxy)-1*H*-1,2,3-benzotriazol-1-yl]methyl}-1*H*-pyrazolo[3,4-*b*]pyridin-6-aminium chloride (7·HCl). A suspension of **7** (48 mg, 0.106 mmol) was treated as in **6**·HCl to give **7**·HCl (52 mg, 100%) as a white solid. ^{1}H NMR (DMSO-d_6 with puff of NH_3 vapor): δ 7.84−7.78 (m, 2H), 7.75 (d, J = 9 Hz, 1H), 7.58 (m, 1H), 7.56 (d, J = 9 Hz, 1H), 7.52 (m, 1H), 6.37 (br s, 2H), 6.30 (d, J = 8.8 Hz, 1H), and 6.16 (s, 2H) ppm. HRMS: measured m/z, $[M + H]^+$ = 451.0577 (theoretical, 451.0584). LC purity 99.7%; t_R = 2.835 min.

4-(3-Bromo-5-chlorophenoxy)-5-chloro-1*H*-benzimidazole (30). A solution of **28** (400 mg, 1.49 mmol) in 90% formic acid (5 mL) was heated to 100 °C for 1 h. This mixture was concentrated in vacuo and then partitioned between EtOAc (40 mL) and saturated aqueous $NaHCO_3$ (40 mL). The organic extract was dried over $MgSO_4$, filtered and the solvent removed in vacuo to give **30** (382 mg, 93%) as a white solid. ^{1}H NMR ($CDCl_3$): δ 8.02 (s, 1H), 7.5 (br s, 1H), 7.40 (d, J = 8.5 Hz, 1H), 7.26 (m, 1H), 6.95 (m, 1H), and 6.83 (m, 1H) ppm. LRMS (M + 1) = 358.7.

3-Chloro-5-[(5-chloro-1*H*-benzimidazol-4-yl)oxy]-benzonitrile (34). **34** was prepared as for **33** using **30** (430 mg, 1.201 mmol) to give **34** (278 mg, 76%) as a white solid. ^{1}H NMR (CD_3OD): δ 8.22 (s, 1H), 7.65−7.50 (m, 2H), 7.49 (br s, 1H), 7.45 (d, J = 8.7 Hz, 1H), and 7.15−7.10 (m, 2H) ppm. LRMS (M + 1) = 303.8.

3-Chloro-5-{[5-chloro-1-(1*H*-pyrazolo[3,4-*b*]pyridin-3-ylmethyl)-1*H*-benzimidazol-4-yl]oxy}benzonitrile Dihydrochloride (8). **34** was treated with **20** as in the synthesis of **3** to give the free base of **8**. The solid was purified by chromatography using silica gel, eluting with 0−10% MeOH/CH_2Cl_2. The pure fractions were combined, treated with 1 N HCl to pH 3 and the solvent was removed in vacuo to provide **8** (46 mg, 29%) as a white solid. ^{1}H NMR (DMSO-d_6): δ 13.7 (s, 1H), 8.58 (s, 1H), 8.52 (d, J = 4.4 Hz, 1H), 8.16 (d, 8.0 Hz, 1H), 7.74 (dd, J = 1.5 Hz, 1H), 7.63 (d, J = 8.8 Hz, 1H), 7.47 (d, J = 8.5 Hz, 1H), 7.39 (dd, J = 1.5 Hz, 1H), 7.29 (dd, J = 2 Hz, 1H), 7.19 (dd, J = 4.5 and 8.1 Hz, 1H), and 5.92 (s, 2H) ppm. HRMS: measured m/z, $[M + H]^+$ = 435.0512 (theoretical, 435.0522). LC purity 96.5%; t_R = 3.090 min.

4-(3-Bromo-5-chlorophenoxy)-5-chloro-1,3-dihydro-2*H*-benzimidazol-2-one (31). To a solution of **28** (204 mg, 0.586 mmol) in DMF (3.5 mL) was added pyridine (119 μL, 1.465 mmol), and the mixture was cooled over an ice bath. This solution was treated with triphosgene (69.6 mg, 0.234 mmol) and stirred at 0 °C for 20 min. The reaction was quenched with water (10 mL) and the mixture acidified with 1 N HCl to pH 3. Extraction was with CH_2Cl_2 (30 mL) with MeOH (at 1 mL to solubilize). The aqueous layer was further extracted with CH_2Cl_2 (20 mL). The combined extracts were washed with water (10 mL), dried over $MgSO_4$, filtered, and the solvent was removed in vacuo. This residue was preabsorbed onto silica gel (1.5 g) and purified by chromatography using silica gel (12 g), eluting with 0−10% MeOH/CH_2Cl_2 to give **31** (147 mg, 67%) as a white solid. ^{1}H NMR ($CDCl_3$): δ 7.40 (m, 2H), 7.22 (t, J = 1.7 Hz, 1H), 7.14 (d, J = 8.3 Hz, 1H), 6.93 (d, J = 8.3 Hz, 1H), 6.93 (t, J = 1.7 Hz, 1H), and 6.82 (t, J = 1.9 Hz, 1H) ppm. LRMS (M + 1) = 374.7.

3-Chloro-5-[(5-chloro-2-oxo-2,3-dihydro-1*H*-benzimidazol-4-yl)oxy]benzonitrile (35). **35** was prepared as for **33** using **31** (147 mg, 0.393 mmol) to give **35** (905 mg, 72%) as a white solid. ^{1}H NMR (DMSO-d_6): δ 11.15 (s, 1H), 10.0 (s, 1H), 7.76 (t, J = 1.5 Hz, 1H), 7.37 (dd, J = 1.2 and 2.4 Hz, 1H), 7.31 (t, J = 2 Hz, 1H), 7.14 (d, J = 8.3 Hz, 1H), and 6.91 (d, J = 8.3 Hz, 1H) ppm. LRMS (M + 1) = 339.0.

3-Chloro-5-{[5-chloro-2-oxo-1-(1*H*-pyrazolo[3,4-*b*]pyridin-3-ylmethyl)-2,3-dihydro-1*H*-benzimidazol-4-yl]oxy}benzonitrile (9). To a solution of **35** (83.9 mg, 0.262 mmol) and **20** (54.0 mg, 0.173 mmol) in DMF (2 mL) at 0 °C was added Cs_2CO_3 (85 mg, 0.262 mmol), and the mixture was stirred for 10 min over an ice bath. Then the mixture was removed from the cooling bath and stirred for an additional 1 h. LC−MS indicates mostly **35** and bis alkylated product with only minor amounts of the 2 monoalkylated products. The mixture was filtered through a Gelman Acrodisc and purified using reverse phase chromatography. The fractions containing the desired monoalkylated product were combined and lyophilized. This residue was dissolved in TFA (3 mL) for 5 min and the solvent was removed in vacuo. This residue was again purified using reverse phase chromatography to give **9** (8.3 mg, 7%) as a white solid. ^{1}H NMR (DMSO-d_6): δ 13.6 (s, 1H), 11.58 (s, 1H), 8.51 (dd, J = 1.5 and 3 Hz, 1H), 8.19 (d, J = 8 Hz, 1H), 7.76 (m, 1H), 7.37 (m, 1H), 7.33 (m, 1H), 7.22 (d, J = 8.5 Hz, 1H), 7.20 (dd, J = 4.4 and 8 Hz, 1H), 7.13 (d, J = 9 Hz, 1H), and 5.34 (s, 2H) ppm. HRMS: measured m/z, $[M + H]^+$ = 451.0466 (theoretical, 451.0474). LC purity 100%; t_R = 3.242 min.

4-(3-Bromo-5-chlorophenoxy)-5-chloro-2-methyl-1*H*-benzimidazole (32). A solution of **28** (204 mg, 0.586 mmol) in AcOH (3.4 mL) was heated to 100 °C for 6 h. The solvent was removed in vacuo, and the residue was partitioned between saturated aqueous $NaHCO_3$ (10 mL) and CH_2Cl_2 (20 mL). The organic extract was dried over $MgSO_4$, filtered, and the solvent was removed in vacuo. This residue was purified by chromatography using silica gel (12 g), eluting with 0−10% MeOH/CH_2Cl_2 to give **32** (217 mg, 99.5%) as a white solid. ^{1}H NMR ($CDCl_3$): δ 7.4 (br s, 1H), 7.33−7.28 (m, 2H), 7.15 (s, 1H), 6.85 (s, 1H), 6.74 (s, 1H), and 2.56 (s, 3H) ppm. LRMS (M + 1) = 372.7.

3-Chloro-5-[(5-chloro-2-methyl-1*H*-benzimidazol-4-yl)oxy]-benzonitrile (36). **36** was prepared as for **33** using **32** (217 mg, 0.583 mmol) to give **36** (129 mg, 69%) as a white solid. ^{1}H NMR (DMSO-d_6): δ 12.66 (s, 1H), 7.73 (t, J = 1.5 Hz, 1H), 7.43 (d, J = 8.5 Hz, 1H), 7.34 (m, 1H), 7.33 (d, J = 8.5 Hz, 1H), 7.22 (t, J = 1.8 Hz, 1H), and 2.5 (s, 3H) ppm. LRMS (M + 1) = 317.8.

3-Chloro-5-{[5-chloro-2-methyl-1-(1*H*-pyrazolo[3,4-*b*]-pyridin-3-ylmethyl)-1*H*-benzimidazol-4-yl]oxy}benzonitrile trifluoroacetate (10). A solution of **36** (104 mg, 0.327 mmol) and **20** (102 mg, 0.327 mmol) in DMF (3 mL) was stirred over an ice bath for 5 min and then treated with Cs_2CO_3 (107 mg, 0.327 mmol) and then stirred at room temperature for 1 h. The mixture was filtered through Gelman Acrodisc and purified using reverse phase chromatography. The desired fractions were combined and lyophilized. This solid was deprotected in TFA (3 mL) for 5 min, and the solvent was removed in vacuo. This residue was again purified using reverse phase chromatography to give **10** (79.2 mg, 43%) as a white solid. ^{1}H NMR (DMSO-d_6): δ 13.75 (s, 1H), 8.52 (dd, J = 1.5 and 4.5 Hz, 1H), 8.02 (d, J = 7.8 Hz, 1H), 7.74 (t, J = 1.5 Hz, 1H), 7.69 (d, J = 8.8 Hz, 1H), 7.42 (d, J = 8.5 Hz, 1H), 7.37 (dd, J = 1.2 and 2.5 Hz, 1H), 7.25 (t, J = 4.5 and 8.2 Hz, 1H), 5.87 (s, 2H), and 2.59 (s, 3H) ppm. HRMS: measured m/z, $[M + H]^+$ = 449.0671 (theoretical, 449.0679). LC purity 100%; t_R = 2.801 min.

3-Chloro-5-[3,5-dichloro-1*H*-indazol-4-yl)oxy]benzonitrile. To a solution of **19** (100 mg, 0.329 mmol) in DMF (1 mL) were added 1.0 M KO^{t}Bu in THF (329 μL, 0.329 mmol) and then NCS (44 mg, 0.329 mmol). The resulting mixture was stirred for 10 min and then purified by reverse phase chromatography to give the title compound (42 mg, 37.8%) as a white solid. ^{1}H NMR (DMSO-d_6): δ 10.1 (s, 1H), 7.54 (d, J = 9 Hz, 1H), 7.40 (d, J = 9 Hz, 1H), 7.35 (m, 1H), 7.15 (m, 1H), and 6.95 (m, 1H) ppm. LRMS (M + 1) = 337.9.

3-Chloro-5-{[3,5-dichloro-1-(1*H*-pyrazolo[3,4-*b*]pyridin-3-ylmethyl)-1*H*-indazol-4-yl]oxy}benzonitrile (11). **11** was prepared as for **8** using 3-chloro-5-[3,5-dichloro-1*H*-indazol-4-yl)oxy]-benzonitrile (42 mg, 0.124 mmol) to give **11** (44 mg, 76%) as a white solid. ^{1}H NMR ($CDCl_3$): δ 8.71 (dd, J = 1.7 and 4.6 Hz, 1H), 8.01 (dd, J = 1.7 and 7.9 Hz, 1H), 7.53 (d, J = 9.0 Hz, 1H), 7.48 (d, J = 9.0 Hz, 1H), 7.33 (m, 1H), 7.25 (m, 1H), 7.10 (m, 1H), 6.91 (m, 1H), and 5.89 (s, 2H) ppm. HRMS: measured m/z, $[M + H]^+$ = 469.0122 (theoretical, 469.0133). LC purity 99.5%; t_R = 4.111 min.

4,5-Dichloro-*N*-(methoxybenzyl)-2-nitroaniline (37). 1,2-Dichloro-4,5-dinitrobenzene (1,86 g, 7.85 mmol) and 4-methoxybenzylamine (2.051 mL, 15.7 mmol) were heated in toluene (10 mL) to 90 °C for 1 h. This mixture was diluted with water (100 mL), and the aqueous layer was extracted with EtOAc (200 mL). The extract was washed with water (75 mL), dried over $MgSO_4$, filtered, treated with silica gel (10 g), and the solvent was removed in vacuo. This preabsorbed solid was purified by chromatography using silica gel (40 g), eluting with 40% CH_2Cl_2/hexanes to provide **37** (2.545 g, 99%) as a red crystalline

solid. ^{1}H NMR ($CDCl_3$): δ 8.30 (s, 1H), 8.24 (br s, 1H), 7.25 (d, J = 8.6 Hz, 2H), 6.98 (s, 1H), 6.92 (d, J = 8.6 Hz, 2H), 4.43 (d, J = 5 Hz, 2H), and 3.83 (s, 3H) ppm.

5-(3-Bromo-5-chlorophenoxy)-4-chloro-*N*-(4-methoxybenzyl)-2-nitroaniline (38). To a suspension of **37** (2.50 g, 7.64 mmol) in NMP (10 mL) was added 3-bromo-5-chlorophenol (3.17 g, 15.28 mmol) and K_2CO_3 (2.112 g, 15.28 mmol). The mixture was heated to 100 °C for 2 h. This mixture was diluted with water (400 mL), and the aqueous layer was extracted with EtOAc (2 × 400 mL). The combined extracts were further washed with water (200 mL) and then brine (100 mL). This solution was dried over MgSO4, filtered and the solvent removed in vacuo. This residue was preabsorbed onto silica gel (13 g) and purified by chromatography using silica gel (80 g), eluting with 10−100% CH_2Cl_2/hexanes to give **38** (2.814 g, 74%) as a solid. ^{1}H NMR ($CDCl_3$): δ 8.49 (m, 1H), 8.33 (s, 1H), 7.39 (t, J = 1.6 Hz, 1H), 7.07 (d, J = 8.8 Hz, 2H), 7.03 (t, J = 2 Hz, 1H), 6.91 (t, J = 2 Hz, 1H), 6.85 (d, J = 8.8 Hz, 2H), 6.17 (s, 1H), 4.29 (d, J = 5.5 Hz, 2H), and 3.81 (s, 3H) ppm.

5-(3-Bromo-5-chlorophenoxy)-4-chloro-2-nitroaniline (39). A solution of **38** (2.814 g, 5.63 mmol) in TFA (20 mL) was heated to reflux for 1 h. The solvent was removed in vacuo, and the residue was partitioned between CH_2Cl_2 (2 × 100 mL) and aqueous Na_2CO_3 (50 mL). This extract was concentrated in vacuo and the residue was purified by chromatography using silica gel (40 g), eluting with 10−100% CH_2Cl_2/hexanes to give **39** (2.125 g, 100%) as a solid. ^{1}H NMR ($CDCl_3$): δ 8.29 (s, 1H), 7.40 (m, 1H), 7.13 (m, 1H), 7.03 (m, 1H), 6.21 (s, 1H), and 6.12 (br s, 2H) ppm.

5-(3-Bromo-5-chlorophenoxy)-4-chloro-2-nitro-*N*-(1*H*-pyrazolo[3,4-*b*]pyridin-3-ylmethyl)aniline (40). To a solution of **39** (81 mg, 0.214 mmol) and **20** (66.9 mg, 0.214 mmol) in DMF (500 μL) was added cesium carbonate (69.8 mg, 0.214 mmol), and the mixture was stirred at room temperature for 4 days. The resulting mixture was partitioned between EtOAc (2 × 10 mL) and water (10 mL). The combined extracts were washed with water (5 mL), dried over $MgSO_4$, filtered, and the solvent was removed in vacuo. This residue was further dried under high vacuum for 24 h to remove excess DMF and then redissolved in TFA (4 mL). This solution was stirred for 30 min, and then the solvent was removed in vacuo. This residue was partitioned between EtOAc (2 × 10 mL) and aqueous $NaHCO_3$ (10 mL). The combined extracts were concentrated in vacuo and then purified by chromatography using silica gel (12 g), eluting with 0−40% EtOAc/CH_2Cl_2 to provide recovered **39** (35 mg, 43%), bis alkylated product (21.2 mg, 15.6%), and **40** (35.3 mg, 32.4%) as a solid. ^{1}H NMR ($CDCl_3$): δ 10.58 (br s, 1H), 8.77 (m, 1H), 8.56 (d, J = 3.1 Hz, 1H), 8.33 (s, 1H), 8.08 (d, J = 7.5 Hz, 1H), 7.42 (t, J = 1.7 Hz, 1H), 7.18 (dd, J = 4.6 and 8.0 Hz, 1H), 7.04 (t, J = 2 Hz, 1H), 6.95 (t, J = 2 Hz, 1H), 6.52 (s, 1H), and 4.73 (s, 2H) ppm. LRMS (M + 1) = 509.3.

3-Chloro-5-{2-chloro-4-nitro-5-[(1*H*-pyrazolo[3,4-*b*]pyridin-3-ylmethyl)amino]phenoxy}benzonitrile trifluoroacetate. To a solution of **40** (35 mg, 0.069 mmol) in DMF (500 μL) was added palladium tetrakistriphenylphosphine (23.8 mg, 0.021 mmol) and $Zn(CN)_2$ (8.07 mg 0.069 mmol). The mixture was heated to 95 °C for 2 h. The reaction was monitored by LC−MS. To the mixture were added additional palladium tetrakistriphenylphosphine (23.8 mg, 0.021 mmol) and $Zn(CN)_2$ (8.07 mg, 0.069 mmol). The mixture was heated to 95 °C for 1 h. The mixture was filtered through a Gelman Acrodisc and purified using reverse phase chromatography to provide recovered **40** (10 mg, 23%) and the title compound (29.6 mg, 76%) as a solid. ^{1}H NMR ($CDCl_3$): δ 8.75 (m, 1H0, 8.53 (d, J = 4.4 Hz, 1H), 8.36 (s, 1H), 8.31 (d, J = 7 Hz, 1H), 7.53 (s, 1H), 7.32 (dd, J = 4.9 and 8.0 Hz, 1H), 7.21 (t, J = 2 Hz, 1H), 7.14 (s, 1H), 6.22 (s, 1H), and 4.80 (d, J = 5.9 Hz, 2H) ppm.

3-{4-Amino-2-chloro-5-[(1*H*-pyrazolo[3,4-*b*]pyridin-3-ylmethyl)amino]phenoxy}-5-chlorobenzonitrile (14). A suspension of 3-chloro-5-{2-chloro-4-nitro-5-[(1*H*-pyrazolo[3,4-*b*]pyridin-3-ylmethyl)amino]phenoxy}benzonitrile trifluoroacetate (29.6 mg 0.052 mmol) and $SnCl_2$ (105 mg, 0.466 mmol) in MeOH (3 mL) was heated to reflux for 1 h. The resulting mixture was allowed to cool to room temperature and diluted with EtOAc (40 mL). This mixture was treated with saturated aqueous Na_2CO_3 (20 mL) and stirred for 30 min. The resulting mixture was partitioned, and the aqueous portion was back-extracted with EtOAc (40 mL). The combined extracts were washed with water (20 mL), dried over $MgSO_4$, filtered, and the solvent was removed in vacuo. This residue was purified by chromatography using silica gel (4 g), eluting with 40−100% EtOAc/CH_2Cl_2 to provide **14** (8.9 mg, 40%) as a solid. ^{1}H NMR ($CDCl_3$): δ 8.57 (d, J = 4.6 Hz, 1H), 8.11 (d, J = 8 Hz, 1H), 7.55−7.50 (m, 1H), 7.26 (m, 1H), 7.16 (dd, J = 4.6 and 8 Hz, 1H), 7.08 (t, J = 2 Hz, 1H), 6.96 (br t, 1H), 6.83 (s, 1H), 6.57 (m, 1H), and 4.63 (s, 2H) ppm. HRMS: measured m/z, $[M + H]^+$ = 425.0679 (theoretical, 425.0679). LC purity 100%; t_R = 2.926 min.

3-Chloro-5-{[5-chloro-1-(1*H*-pyrazolo[3,4-*b*]pyridine-3-ylmethyl)-1*H*-1,2,3-benzotriazol-6-yl]oxy}benzonitrile (12). A solution of **14** (0.96 mg, 0.0023 mmol) in AcOH (200 μL) was treated with a solution of $NaNO_2$ (0.23 mg, 0.0034 mmol) in water (200 μL), and the mixture was stirred for 10 min. The solvent was removed in vacuo and the residue was purified by reverse phase chromatography and lyophilized to give **12** (0.95 mg, 96%) as a solid. ^{1}H NMR (CD_3OD): δ 8.50 (d, J = 4.5 Hz, 1H), 8.24 (s, 1H), 8.14 (d, J = 8 Hz, 1H), 7.60 (m, 1H), 7.58 (s, 1H), 7.29 (m, 1H), 7.27 (m, 1H), 7.19 (dd, J = 4.5 and 8 Hz, 1H), and 6.27 (s, 2H) ppm. HRMS: measured m/z, $[M + H]^+$ = 436.0466 (theoretical, 436.0475). LC purity 100%; t_R = 3.474 min.

3-Chloro-5-{[5-chloro-1-(1*H*-pyrazolo[3,4-*b*]pyridine-3-ylmethyl)-1*H*-benzimidazol-6-yl]oxy}benzonitrile trifluoroacetate (13). A solution of **14** (0.96 mg, 0.0023 mmol) in formic acid (500 μL) was heated to 100 °C for 1 h. This mixture was evaporated in vacuo and the residue was purified by reverse phase chromatography and lyophilized to give **13** (1.05 mg, 85%) as a solid. ^{1}H NMR (DMSO-d_6): δ 13.68 (s, 1H), 8.74 (s, 1H), 8.51 (d, J = 4,4 Hz, 1H), 8.16 (d, J = 8.2 Hz, 1H), 7.98 (s, 1H), 7.78 (t, J = 1.6 Hz, 1H), 7.74 (s, 1H), 7.42 (m, 1H), 7.33 (t, J = 2.1 Hz, 1H), 7.17 (dd, J = 4.5 and 8.1 Hz, 1H), and 5.89 (s, 2H) ppm. HRMS: measured m/z, $[M + H]^+$ = 435.0513 (theoretical, 435.0522). LC purity 99%; t_R = 2.800 min.

■ AUTHOR INFORMATION

Corresponding Author

*Phone: 215-652-4715. Fax: 215-652-3971. E-mail: Robert_gomez@merck.com.

Present Addresses

●Department of Boston Discovery Chemistry, Merck Research Labs., 33 Avenue Louis Pasteur, Boston, Massachusetts 02115-5717, United States.

■ ACKNOWLEDGMENTS

The authors thank Dr. Steve Young for his guidance and support and Elizabeth Cauchon, Manuel Chan, Wanda Cromlish, and Sebastian Guiral for their assistance in acquiring necessary data for publication.

■ ABBREVIATIONS USED

HAART, highly active antiretroviral therapy; HIV, human immunodeficiency virus; AIDS, acquired immunodeficiency syndrome; NNRTI, non-nucleoside reverse transcriptase inhibitor; wt, wild type; RT, reverse transcriptase; NRTI, nucleoside reverse transcriptase inhibitor; ΔE, change in energy; CIC_{95}, cell inhibitory concentration that blocks 95% of cell replication; FBS, fetal bovine serum; NHS, normal human serum; EFV, efavirenz; iv, intravenous; nAUC, normalized area under the plasma concentration vs time curve; V_d, volume of distribution; Cl_p, plasma clearance; $t_{1/2}$, half-life; F, bioavailability

REFERENCES

(1) Coffin, J. M. Genetic variation in AIDS viruses. *Cell* **1986**, *46* (1), 1−4.

(2) Perrino, F. W.; Preston, B. D.; Sandell, L. L.; Loeb, L. A. Extension of mismatched 3′ termini of DNA is a major determinant of the infidelity of human immunodeficiency virus type 1 reverse transcriptase. *Proc. Natl. Acad. Sci. U.S.A.* **1989**, *86* (21), 8343−8347.

(3) Menendez-Arias, L. Molecular basis of fidelity of DNA synthesis and nucleotide specificity of retroviral reverse transcriptases. *Prog. Nucleic Acid Res. Mol. Biol.* **2002**, *71*, 91−147.

(4) Gulick, R. M.; Mellors, J. W.; Havlir, D; Eron, J. J.; Meibohm, A.; Condra, J. H.; Valentine, F. T.; McMahon, D.; Gonzalez, C.; Jonas, L.; Emini, E. A.; Chodakewitz, J. A.; Isaacs, R.; Richman, D. D. 3-Year suppression of HIV viremia with indinavir, zidovudine, and lamivudine. *Ann. Intern. Med.* **2000**, *133* (1), 35−39.

(5) Cane, P. A. New developments in HIV drug resistance. *J. Antimicrob. Chemother.* **2009**, *64* (Suppl. 1), i37−i40.

(6) Little, S. J.; Holte, S.; Routy, J.-P.; Daar, E. S.; Markowitz, M.; Collier, A. C.; Koup, R. A.; Mellors, J. W.; Connick, E.; Conway, B.; Kilby, M.; Wang, L.; Whitcomb, J. M.; Hellmann, N. S.; Richman, D. D. Antiretroviral-drug resistance among patients recently infected with HIV. *N. Engl. J. Med.* **2002**, *347* (6), 385−394.

(7) Richman, D. D.; Morton, S. C.; Wrin, T.; Hellmann, N.; Berry, S.; Shapiro, M. F.; Bozzette, S. A. The prevalence of antiretroviral drug resistance in the United States. *AIDS (London)* **2004**, *18* (10), 1393−1401.

(8) de Bethune, M.-P. Non-nucleoside reverse transcriptase inhibitors (NNRTIs), their discovery, development, and use in the treatment of HIV-1 infection: a review of the last 20 years (1989−2009). *Antiviral Res.* **2010**, *85* (1), 75−90.

(9) Sluis-Cremer, N.; Temiz, N. A.; Bahar, I. Conformational changes in HIV-1 reverse transcriptase induced by nonnucleoside reverse transcriptase inhibitor binding. *Curr. HIV Res.* **2004**, *2* (4), 323−232.

(10) Fokunang, C. N.; Hitchcock, J.; Spence, F.; Tembe-Fokunang, E. A.; Burkhardt, J.; Levy, L.; George, C. An overview of mitochondrial toxicity of nucleoside reverse transcriptase inhibitors associated with HIV therapy. *Int. J. Pharmacol.* **2006**, *2* (1), 152−162.

(11) Cheung, P. K; Wynhoven, B.; Harrigan, P. R. Which HIV-1 drug resistance mutations are common in clinical practice? *AIDS Rev.* **2004**, *6* (2), 107−116.

(12) Tambuyzer, L.; Azijn, H.; Rimsky, L. T.; Vingerhoets, J.; Lecocq, P.; Kraus, G.; Picchio, G.; de Bethune, M.-P. Compilation and prevalence of mutations associated with resistance to non-nucleoside reverse transcriptase inhibitors. *Antiviral Ther.* **2009**, *14* (1), 103−109.

(13) Das, K.; Clark, A. D. Jr.; Lewi, P. J.; Heeres, J.; De Jonge, M. R.; Koymans, L. M. H.; Vinkers, H. M.; Daeyaert, F.; Ludovici, D. W.; Kukla, M. J.; De Corte, B.; Kavash, R. W.; Ho, C. Y.; Ye, H.; Lichtenstein, M. A.; Andries, K.; Pauwels, R.; De Bethune, M.-P.; Boyer, P. L.; Clark, P.; Hughes, S. H.; Janssen, P. A. J.; Arnold, E. Roles of conformational and positional adaptability in structure-based design of TMC125-R165335 (etravirine) and related non-nucleoside reverse transcriptase inhibitors that are highly potent and effective against wild-type and drug-resistant HIV-1 variants. *J. Med. Chem.* **2004**, *47* (10), 2550−2560.

(14) Arasteh, K.; Riege, R. A.; Yeni, P.; Pozniak, A.; Boogaerts, G.; van Heeswijk, R.; de Bethune, M.-P.; Peeters, M.; Woodfall, B. Short-term randomized proof-of-principle trial of TMC278 in patients with HIV type-1 who have previously failed antiretroviral therapy. *Antiviral Ther.* **2009**, *14* (5), 713−722.

(15) Tucker, T. J.; Sisko, J. T.; Tynebor, R. M.; Williams, T. M.; Felock, P. J.; Flynn, J. A.; Lai, M.-T.; Liang, Y.; McGaughey, G.; Liu, M.; Miller, M.; Moyer, G.; Munshi, V.; Perlow-Poehnelt, R.; Prasad, S.; Reid, J. C.; Sanchez, R.; Torrent, M.; Vacca, J. P.; Wan, B.-L.; Yan, Y. Discovery of 3-{5-[(6-amino-1*H*-pyrazolo[3,4-*b*]pyridine-3-yl)-methoxy]-2-chlorophenoxy}-5-chlorobenzonitrile (MK-4965): a potent, orally bioavailable HIV-1 non-nucleoside reverse transcriptase inhibitor with improved potency against key mutant viruses. *J. Med. Chem.* **2008**, *51* (20), 6503−6511.

(16) De Luca, S.; Saviano, M.; Della Moglie, R.; Digilio, G.; Bracco, C.; Aloj, L.; Tarallo, L.; Pedone, C.; Morelli, G. Conformationally constrained CCK8 analogues obtained from a rationally designed peptide library as ligands for cholecystokinin type B receptor. *ChemMedChem.* **2006**, *1* (9), 997−1006.

(17) Hruby, V. J.; Al-Obeidi, F.; Kazmierski, W. M. Emerging approaches in the molecular design of receptor selective peptide ligands: conformational, topographical and dynamic considerations. *Biochem. J.* **1990**, *268*, 249−262.

(18) The low mode/mixed-torsional sampling algorithm as implemented in software from Schrodinger, LLC, version 2009.1, was used with a distance dependent dielectric constant of 2 with the MMFFs force field to determine the lowest energy conformer. The protein−ligand complex was minimized using the same force field and parameters.

(19) Full experimental protocols for the HIV-1 RT polymerase SPA assay are described in the following patent application: Saggar, S. A.; Sisko, J. T.; Tucker, T. J.; Tynebor, R. M.; Su, D.-S.; Anthony, N. J. Preparation of Heterocyclic Phenoxy Compounds as HIV Reverse-Transcriptase Inhibitors. U.S. Patent Appl. US 2007/021442 A1, 2007.

(20) Vacca, J. P.; Dorsey, B. D.; Schleif, W. A.; Levin, R. B.; McDaniel, S. L.; Darke, P. D.; Zugay, J.; Quintero, J. C.; Blahy, O. M.; Roth, E.; Sardana, V. V.; Schlabac, A. J.; Graham, P. I.; Condra, J. H.; Gotlib, L.; Holloway, M. K.; Lin, J.; Chen, I.-W.; Vastag, K.; Ostovic, D.; Anderson, P. S.; Emini, E. E.; Huff, J. R. L-735,524: an orally bioavailable human immunodeficiency virus type 1 protease inhibitor. *Proc. Natl. Acad. Sci. U.S.A.* **1994**, *91*, 4096−4100.

(21) The X-ray diffraction data of the wt RT and inhibitor **5** complex crystal (Figure 4) were obtained at 2.6 Å resolution and refined to an *R*-factor of 0.199 and an R_{free} of 0.248. The X-ray diffraction data of the K103N mutant RT and inhibitor **5** complex crystal were obtained at 2.4 Å and refined to an *R*-factor of 0.207 and an R_{free} of 0.250. Both structures are deposited in the Protein Data Bank: 3T19 (wild type) and 3T1A (K103N mutant).

(22) Sweeney, Z. H.; Harris, S. F.; Arora, N; Javanbakht, H.; Li, Y.; Fretland, J.; Davidson, J. P.; Billedeau, J. R.; Gleason, S. F.; Hirschfeld, D.; Kennedy-Smith, J. J.; Mirzadegan, T.; Roetz, R.; Smith, M.; Sperry, S.; Suh, J.; Wu, J.; Tsing, S.; Villaseñor, A. G.; Paul, A.; Su, G.; Heilek, G.; Hang, J. Q.; Zhou, A. S.; Jernelius, J. A.; Zhang, F.-J.; Klumpp, K. Design of annulated pyrazoles as inhibitors of HIV-1 reverse transcriptase. *J. Med. Chem.* **2008**, *51* (23), 7449−7458.

(23) Jones, L.; Allan., G.; Barba, O.; Burt., C.; Corbau, R.; Dupont, T.; Knöchel.; Irving, S.; Middleton, D. S.; Mowbray, C. E.; Perros, M.; Ringrose, H.; Swain, N. A.; Webster, R.; Westby, M.; Phillips, C. Novel indazole non-nucleoside reverse transcriptase inhibitors using molecular hybridization based on crystallographic overlays. *J. Med. Chem.* **2009**, *52* (4), 1219−1223.

(24) The compounds were evaluated in a Monogram Bioscience Phenosense assay versus a panel of clinically derived RT mutants in the presence of 10% FBS. The IC_{50} is defined as the concentration of compound in cell culture required to block 50% of viral replication. Values are derived from the average of two determinations. Assays were performed by Monogram Biosciences, South San Francisco, CA. Details of the assay protocols are available at http://www.monogramhiv.com/phenosense_introduction.aspx.

(25) Dykes, C.; Demeter, L. M. Y188H, Which Is a Potential Intermediate between Wild-Type (WT) and Y188L, Has Markedly Reduced Replication Efficiency. Presented at the 14th Conference on Retroviruses and Opportunistic Infections, Los Angeles, CA, Feb 25−28, 2007; Poster 633.

(26) pK_a prediction using ACD/pKa DB from Phys/Chem Suite by Advanced Chemical Development, Inc. The base compound, *N*-methylbenzimidazole, has a pK_a of 5.40. Substituent effects using the Dewar-Grisdale method is calculated at −1.733, giving **8** a predicted pK_a of 3.667.

(27) Grzegozek, M. Vicarious nucleophilic amination of nitroquinolines by 1,1,1-trimethylhydrazinium iodide. *J. Heterocycl. Chem.* **2008**, *45* (6), 1879−1882.